IEEE Access
Multidisciplinary | Rapid Review | Open Access Journal

Received 9 January 2024, accepted 29 January 2024, date of publication 20 February 2024, date of current version 29 February 2024.

Digital Object Identifier 10.1109/ACCESS.2024.3368383

RESEARCH ARTICLE

Comparative Analysis of Nature-Inspired Algorithms for Optimal Power Flow Problem: A Focus on Penalty-Vanishing Terms and Algorithm Performance

GERARDO CASTAÑÓN[1], (Senior Member, IEEE), ALBERTO F. MARTÍNEZ-HERRERA[1], (Member, IEEE), ANA MARIA SARMIENTO[1], (Member, IEEE), ALEJANDRO ARAGÓN-ZAVALA[2], (Senior Member, IEEE), AND FERNANDO LEZAMA[3], (Senior Member, IEEE)

[1]School of Engineering and Sciences, Tecnológico de Monterrey, Monterrey, Nuevo Leon 64849, Mexico
[2]Department of Electronics and Mechatronics, Tecnológico de Monterrey, Querétaro Campus, Santiago de Querétaro, Querétaro 76130, Mexico
[3]GECAD—Research Group on Intelligent Engineering and Computing for Advanced Innovation and Development, LASI—Intelligent Systems Associate Laboratory, Polytechnic of Porto, 4200-072 Porto, Portugal

Corresponding author: Fernando Lezama (flz@isep.ipp.pt)

This work was supported by GECAD Research Center under Grant UIDB/00760/2020, DOI: 10.54499/UIDB/00760/2020.

ABSTRACT This study presents a comparative analysis of multiple nature-inspired algorithms for solving the non-polynomial Optimal Power Flow (OPF) problem. Through numerical evaluations, we assess their performance across diverse objective functions, addressing complexities such as multi-fuel sources, valve point effects, and prohibited zones. The study involves the implementation of different nature-inspired heuristics and variants of the differential evolution algorithm to analyze their efficacy in solving the OPF problem within the context of large networks, specifically IEEE-30 and IEEE-57. The objectives of this research are threefold: (i) to determine the most effective nature-inspired algorithms for each case under consistent constraints, initial conditions, and using optimized parameters, (ii) to assess the success rate of penalty-vanishing terms concerning the penalized function versus the actual objective function, and (iii) to explore the impact of minor variations within a network on the behaviors, results, and profiles of penalty-vanishing terms. Utilizing a low-high sorting ranking method, considering mean, maximum, and minimum values for result computation and sorting, we identify the optimal algorithm among all those assessed for various objective functions, alongside assessing the success rate of penalty-vanishing terms. Our findings reveal that the differential evolution algorithm best version (DEAB) emerges as the most valuable solution.

INDEX TERMS Nature-inspired algorithms, optimal power flow, optimization, penalty-vanishing terms, success rate.

I. INTRODUCTION

The Optimal Power Flow (OPF) problem is the most used to analyze an electric network to obtain efficient operation conditions with the lowest cost [1] or the minimum power loss [2] with classical optimization approaches [3]. Since the 90s, this problem has been analyzed with nature-inspired algorithms [4], and since then, the trend has been strengthened to obtain different ways of improving the performance of electric networks. Most of the work in the literature is mainly focused on reducing the monetary costs (in $/h), the power losses (in MW), the pollutant emissions (in ton/h), the voltage instability (in p.u.), combinations of these factors, among other applications [5].

In this study, we explore several established nature-inspired algorithms applied to address the Optimal Power Flow (OPF)

The associate editor coordinating the review of this manuscript and approving it for publication was Ali Raza.

problem, aiming to conduct a comparative analysis. Our research contributes to the field in the following ways: firstly, by identifying which of the tested nature-inspired algorithms perform best for each case under consistent constraints and initial conditions; secondly, by assessing the success rate of the penalty-vanishing process within the penalized function concerning the actual objective function; and lastly, by delving into how even slight variations within a given network can result in divergent penalty-vanishing behaviors, outcomes, and profiles. Our evaluation includes four variants of the Differential Evolution (DE) algorithm, alongside other well-established nature-inspired algorithms: Particle Swarm Optimization (PSO) [6], Teaching Learning Optimization (TL) [7], Bio-geographical Based Optimization (BBO) [8], and Artificial Bee Colony Optimization (ABC) [9]. The comparative evaluation of these algorithms via numerical experiments using optimized parameters is, to the best of the authors knowledge, entirely novel, challenging to execute, and significantly useful. Each algorithm is tailored to address standard objective functions and optimal parameters as documented in existing literature for OPF problem solving. Employing the methodology outlined by Castañón et al. [10], we rank the tested nature-inspired algorithms through a low-high sorting ranking. Additionally, we calculate a success rate ranking to identify the best-performing algorithm. This provides a baseline to determine the behaviors of the analyzed meta-heuristics before using them in more elaborated scenarios where valve-point loading effects, prohibited operating zones, and similar conditions are considered. Each meta-heuristic is evaluated on the success rate of penalty-vanishing functions and by the mean, minimum, and maximum values obtained. It is well-known that the classic/analytical optimization methods (Lagrange, Linear Programming, etc.) are not able to hold problems with non-convex/non-smooth nature or they have non-differentiable points, especially where multi-fuel sources, prohibited operating zones, and valve point effects are included [11].

This work is organized as follows: Section II presents the state of the art related to OPF. Section III shows a description and the mathematical statement of the OPF. Section IV presents a detailed description of the objective functions to be used and their versions with penalization factors. Section V describes the DE algorithm and its variants tested throughout this manuscript. Section IX describes the electric networks tested as given scenarios. Section VI describes the methodology to apply the used nature-inspired algorithms to the scenarios described in Section IX. Section VII describes the results obtained with the nature-inspired algorithms to determine the ranking. Section VIII presents a discussion of the results, and finally, Section IX summarizes the conclusions and open problems.

II. STATE OF THE ART

This section reviews some of the different applications and research in OPF and meta-heuristics. The nomenclature of the objective functions and definitions mentioned in this paper are shown in Table 1. Please refer to Table 2 at the end of this section for a summary of the review presented next.

TABLE 1. Nomenclature of the objective functions.

Abrevation	Definition
MC	Monetary fuel costs.
VP	Voltage profile.
VSLI	Voltage Stability or L_{index} factor.
PWQC	Piecewise Quadratic Cost.
PL	Power loss.
POZ	Prohibited zones.
V/P	Valve-Point.
PE	Pollutant emissions.
PEM	Pollutant emissions Modified.
V/P|PWQC	Valve point mixed with piecewise quadratic costs.
V/P|PWQC|Tie	Valve point mixed with piecewise quadratic costs and tie factors.
V/P|POZ	Valve point mixed with prohibited zones.

In prior work, Osman et al. [12] used a classical genetic algorithm (GA) on a 6-bus example [13] to determine the MC of the network. Pérez-Guerrero et al. [14] introduced a multi-objective version of DE that considers costs, V/P effects and the PE, within the IEEE-30 network, employing DE/best/2/bin as the variant. Yang et al. [15] explored different DE versions for optimizing a combination of PL and VSLI objective functions and introduced a DE variant with fitness sharing, validated against Schwefel's Function. All these DE variants were tested on the IEEE-57 network.

Noman and Iba [16] conducted a comprehensive study to analyze the impact of various parameters on standard DE versions when applied to objective functions involving MC, PWQC, and V/P. Notably, they introduced non-conventional electric networks (SYS-1 to SYS-5) for their analysis, encompassing small, medium, and large electric networks, distinguishing their work from prior studies.

Abou et al. [17] used a classical DE approach, similar to Abido [18]; to tackle a range of objective functions, including MC, MC with VP, MC with VSLI, and PWQC. Their testing was performed on the IEEE-30 network, varying populations (e.g., 10, 50, and 100) and introducing compensatory shunt elements at specific positions. They also conducted a complementary study [19] focused on PL, VP, and VSLI problems, evaluating each objective function independently. Additionally, Bhattacharya et al. applied BBO to the IEEE-30 network, addressing six objective functions, such as MC, VP, VSLI, PWQC, MC with VP, and MC with VSLI.

Amjady and Sharifzadeh [20] introduced a multi-objective robust DE variant to address POZ in the presence of V/P effects and multi-fuel options. They enhanced DE by incorporating auxiliary adjusters, optimizing the mutation/recombination process for rapid global convergence. These adjusters utilized roulette wheel selection and alternative subtraction operations in place of classical DE recombination. Their primary objective function integrated V/P effects with POZ considerations, further modified by a

VSLI function V/P|POZ(1+VSLI). They tested this approach on diverse electric networks, including a 26-bus network (26-B), IEEE-30, New England network with 39 buses (NE-39), and IEEE-118.

Sivasubramani and Swarup [21] modified DE, incorporating sequential quadratic programming (SQP) to mitigate issues related to premature convergence and global population addressing. Their objective functions focused on solving PL, V/P effects, and MC for electric networks, including IEEE-30 and IEEE-118 (large size). Niknam et al. [22] combined PL, VSLI, MC, and PE into a single multi-objective function, solved using a modified PSO, with Pareto Front charts to determine the optimal solution within the IEEE-30 network. In another work, Niknam et al. [11] proposed a combination of the Shuffle Frog Leaping Algorithm (SFLA) and Simulated Annealing (SA) to address four objective functions, including MC, V/P, POZ, and V/P|POZ, for the IEEE-30 electric network.

Adaryani and Karami [23] applied ABC to solve individual objective functions, including PL and PE, along with combinations like VP plus PWQC and PWQC plus VSLI. Their tests encompassed electric networks following the IEEE architecture, ranging from IEEE-9 (small size), IEEE-30 (medium size), to IEEE-57 (large size), demonstrating scalability. Vo et al. [24] enhanced the PSO method to independently evaluate MC, V/P, and PWQC across the IEEE electric network family. They showed the scalability of their solution on networks of varying sizes, such as IEEE-14, IEEE-30, IEEE-57, and IEEE-118. In another approach, Bouchekara et al. [25] utilized TL optimization techniques to address MC, PWQC, and V/P on the IEEE-30 and IEEE-118 networks. They also tackled the combined objectives of MC plus VP and MC plus VSLI, following the approach presented by Abou et al. [17].

Ghasemi et al. [26] combined Master-Teacher (MT) and DE bio-inspired methods to assess power loss (PL) in three electric networks: IEEE-14, IEEE-30 (medium size), and IEEE-118 (large size). In another study, Ghasemi et al. [27] improved various bio-inspired methods, creating new hybrid methods applied to diverse objective functions after rigorous feasibility testing. The most effective combination, known as the hybridized sum-local search optimizer, was a blend of DE and PSO. They evaluated these methods across scenarios: 2 areas and 4 generators (2A4G), 4 areas and 16 generators (4A16G), and 2 areas and 40 generators (2A40G), using a mixed objective function comprising V/P, PWQC, and tied factors (Tie).

Shaheen et al. [29] conducted a comprehensive study of large electric networks, focusing on DE, both single and multi-objective approaches, applied to IEEE-30 and IEEE-57 networks. Their analysis covered MC, VP, VSLI, and PL individually, followed by multi-objective testing for combinations like MC plus VP, MC plus VSLI, and MC plus PL. Similarly, Abaci and Yamacli [31] followed a similar approach as Shaheen et al. [29] utilizing a Differential Search Algorithm. They applied their analysis to IEEE-9, IEEE-30, and IEEE-57 networks, evaluating single objective functions for MC, PL, and PE, along with multi-objective objectives MC plus VSLI and MC plus VP. In a different context, Singh and Srivastava [30] used DE to address a combination of PL plus VP in the 75-bus Indian electric network (75-B Indian/net) and the IEEE-30 network.

Basu introduced an extended 3D version of multi-objective DE [32], where DE was initially applied individually to each objective function (PL, VP, VSLI). Subsequently, these functions were combined to determine the optimal outcomes across electric networks, including IEEE-30, IEEE-57 (medium size), and IEEE-118 (large size). Additionally, Warid et al. employed the JAYA (Sanskrit in origin, it means "victory") method to address MC, PL, and VSLI objectives separately in electric networks such as IEEE-30 (medium size) and IEEE-118 (large size), with the novelty lying in the application method.

In [34], an enhanced adaptive DE algorithm (JADE) with a self-adaptive penalty constraint handling technique (EJADE-SP) is introduced. The IEEE 30-bus test system is used to minimize various objectives, such as generation MC, real PL, VP, PE, and MC+PE. Naderi et al. [35] propose a fuzzy adaptive hybrid configuration (FAHSPSO-DE) to optimize power systems, combining Self-Adaptive PSO and DE algorithms. They apply a multi-objective approach to IEEE 30-, 57-, and 118-bus test systems, aiming to minimize total fuel MC while considering V/P, PL, and PE. In [36], a combination of the superiority of feasible solutions (SF) for constraint handling, the fast and elitist multi-objective genetic algorithm (NSGA-II), and adaptive crossover non-dominated sorting differential evolution (ACNSDE) are employed in a multi-objective context. Testing is done on the IEEE-30 and IEEE-57 bus systems, optimizing objectives like MC, PL, and PE.

Kahraman et al. [37] introduced the Improved Multi-Objective Manta-Ray Foraging Optimization (IMOMRFO) algorithm, tailored for solving multi-objective optimization problems. They applied this method to the IEEE 30-bus and 57-bus test systems, optimizing various objectives, including MC, PE, VP, and PL. In [38], a hybridization of the Whale Optimization Algorithm (WOA) and a modified Moth-Flame Optimization algorithm (MFO), known as WMFO, was utilized for both single and multi-objective OPF problems. Testing covered various systems, such as IEEE 14-bus, IEEE 30-bus, IEEE 39-bus, IEEE 57-bus, and IEEE 118-bus, targeting objectives like total fuel MC and VP. Furthermore, [39], introduced the Modified Moth-Flame Optimization and Gradient-Based Optimizer (GBO-MFO) as a multi-objective optimization algorithm. Their approach, applied to the IEEE 30-bus system, focused on minimizing thermal unit fuel costs and wind energy cost estimation while simultaneously reducing MC and PL.

Remarkably, all these existing solutions available in the open literature use the penalty-factor approach to help solve the respective optimization problem by minimizing the complexity of operations. This indicates that it is

TABLE 2. Summary of the cited cases in this manuscript.

Ref.	Method	Approach	Network	Problem
[12]	GA	SI	6-B	MC
[14]	DE	MO	IEEE-30	V/P+PE
[15]	DE	MO	IEEE-57	PL+VSLI
[16]	DE	SI	SYS-1, SYS-2, SYS-3, SYS-4, SYS-5	MC, PWQC, V/P
[17]	DE	SI, MO	IEEE-30	MC, MC+VP MC+VSLI, PWQC
[19]	DE	SI	IEEE-30	PL, VP, VSLI,
[28]	BBO	SI, MO	IEEE-30	MC, VP, VSLI, PWQC, V/P, MC+VP, MC+VSLI
[20]	DE	MO	26-B, IEEE-30, NE-39, IEEE-118	V/P|POZ(1+VSLI)
[21]	DE+SQP	SI	IEEE-30, IEEE-118	PL, V/P, MC
[22]	PSO	MO	IEEE-30	PL+VSLI+MC+PE
[11]	SFLA+SA	SI	IEEE-30	MC, V/P, POZ, V/P|POZ
[23]	BCO	SI, MO	IEEE-9, IEEE-30, IEEE-57	PWQC+VP, PWQC+VSLI, PL, PE
[24]	IPSO	SI	IEEE-14, IEEE-30, IEEE-57, IEEE-118	MC, V/P, PWQC
[25]	TL	MO	IEEE-30, IEEE-118	MC, MC+VP, MC+VSLI, PWQC, V/P
[26]	MT+DE	SI	IEEE-14, IEEE-30, IEEE-118	PL
[27]	DE+PSO	SI, MO	2A4G, 4A16G, 2A40G	V/P|PWQC|Tie, PEM V/P|PWQC|Tie+PEM
[29]	DE	MO	IEEE-30, IEEE-57	MC, VP, VSLI, PL, MC+VP, MC+VSLI, MC+PL
[30]	DE	MO	75-B Indian/net, IEEE-30	PL+VP
[31]	DSA	SI, MO	IEEE-9, IEEE-30, IEEE-57	MC, PL, PE, MC+VSLI, MC+VP
[32]	DE	SI, MO	IEEE-30, IEEE-57, IEEE-118	PL, VP, VSLI, PL+VP+VSLI
[33]	JAYA	SI	IEEE-30, IEEE-118	MC, PL, VSLI
[34]	EJADE-SP	SI	IEEE-30	MC, PL, VP, PE, MC+PE
[35]	FAHSPSO-DE	MO	IEEE-30, IEEE 57, IEEE-118	MC + V/P + PL + PE
[36]	SF + NSGA-II + ACNSDE	MO	IEEE-30, IEEE-57	MC, PL, PE
[37]	IMOMRFO	MO	IEEE-30, IEEE-57	MC, PE, VP, PL
[38]	WMFO	SI, MO	IEEE-14, IEEE-30, IEEE-39, IEEE-57, IEEE-118	MC + VP
[39]	GBO-MFO	MO	IEEE-30	MC + PL

easier to include the constraints like penalty factors as a complementary issue to the original objective function rather than checking each constraint every time a new candidate solution is evaluated. Further insights on the use of penalty factors are provided in this paper.

Table 2 summarizes the references cited to show the various applications, nature-inspired methods, and approaches used in OPF-like problems. The taxonomy is as follows:

- The first column shows the reference number of the work cited.
- The second column refers to the nature-inspired algorithm used by the authors (definition of the abbreviations are given before in this section).
- The third column presents the approach taken in terms of the number of objective functions and their combination:
  - Single (SI). One function is solved, generating one output and the respective solution vector.
  - Multi-Objective (MO). More than one function is solved simultaneously, generating the respective output for each function and the respective solution vector. In Table 2, such a combination is represented as $A + B$. For instance, $MC + VSLI$ means to optimize monetary fuel costs and the voltage stability function at the same time.
- The fourth column presents the network considered.
- The last column refers to the objective function considered in the OPF problem

III. DESCRIPTION OF THE OPF

In this section, we provide the general mathematical formulation of the OPF problem. Subsequent sections specify additional considerations and constraints related to the algorithms for solving it. To enhance clarity, we present the

general formulation here and discuss each modified case in its respective section. The OPF is defined as follows:

$$\text{Minimize} : f(\mathbf{x}, \mathbf{u}) \tag{1}$$

s.t. :

$$g(\mathbf{x}, \mathbf{u}) = 0 \tag{2}$$

$$h(\mathbf{x}, \mathbf{u}) \leq 0 \tag{3}$$

$$\mathbf{x} = [p_{G1}\ \mathbf{V}_L\ \mathbf{Q}_G\ \mathbf{S}_l] \tag{4}$$

$$\mathbf{u} = [\mathbf{P}_G\ \mathbf{V}_G\ \mathbf{Q}_C\ \mathbf{T}_N] \tag{5}$$

where $h(\mathbf{x}, \mathbf{u})$ are the operational constraints of the network, $g(\mathbf{x}, \mathbf{u})$ is the function related to the equilibrium state of the network (i.e. the Kirchhoff's Laws, described below), $\mathbf{x}$ is the vector of values to be computed i.e. dependant variables, $\mathbf{u}$ is the vector of values to be assigned/modified by a heuristic algorithm i.e. independent variables, G is the label of a generator, C is the label of a capacitor, N is the label of the tap, L is the label of a load bus and l is the label of a load line [17], [18], [19].

The elements of $\mathbf{x}$ and $\mathbf{u}$ are [17], [18], and [19]:

- $\mathbf{P}_G$ is a vector: Real power injected to the network, being $\mathbf{P} = [p_{G2}, \ldots, p_{GNG}]$.
- p_{G1} is the power obtained in the node identified as the slack bus.
- $\mathbf{V}_G$ is a vector: Voltage magnitude to the network, being $\mathbf{V}_G = [v_{G1}, \ldots, v_{GNG}]$.
- $\mathbf{Q}_C$ is a vector: Reactive power injected with a shunt device, being $\mathbf{Q}_C = [q_{C1}, \ldots, q_{CNC}]$.
- $\mathbf{Q}_G$ is a vector: Reactive power injected to the network, being $\mathbf{Q}_G = [q_{G1}, \ldots, q_{GNG}]$.
- $\mathbf{T}_N$ is a vector: Tap of the transformer, being $\mathbf{T}_N = [t_1, \ldots, t_{NT}]$.
- $\mathbf{V}_L$ is a vector: Voltage magnitude of the load buses, being $\mathbf{V}_L = [v_{L1}, \ldots, v_{LNL}]$.
- $\mathbf{S}_l$ is a vector: Total power that a load line can hold, being $\mathbf{S}_l = [s_{l1}, \ldots, s_{lnl}]$.

Each vector component constraint is treated as follows:

- Generator constraints (NG being the number of voltage generators).

$$v_{Gm}^{min} \leq v_{Gm} \leq v_{Gm}^{max} \tag{6}$$

$$p_{Gm}^{min} \leq p_{Gm} \leq p_{Gm}^{max} \tag{7}$$

$$q_{Gm}^{min} \leq q_{Gm} \leq q_{Gm}^{max} \tag{8}$$

  where $m \in \{1, .., NG\}$, min, max are the lower and upper values for the corresponding variables, respectively.
- Transformer constraints (NT is the number of taps).

$$t_m^{min} \leq t_m \leq t_m^{max} \tag{9}$$

  where $m \in \{1, .., NT\}$.
- Shunt constraints (NC the number of shunts).

$$q_{Cm}^{min} \leq q_{Cm} \leq q_{Cm}^{max} \tag{10}$$

  where $m \in \{1, .., NC\}$.
- Security constraints.

$$v_{Lm}^{min} \leq v_{Lm} \leq v_{Lm}^{max} \tag{11}$$

$$s_{ln} \leq s_{ln}^{max} \tag{12}$$

  where $m \in \{1, .., NL\}$, NL is the of load buses in the network, $n \in \{1, .., nl\}$, nl is the number of branches of the electric network, $s_n^l = |p_n^l + jq_n^l|$. That means s_n^l must be lower than the power allowed on each network branch.

Given the aforementioned conditions, the most important issue is that the network must be in equilibrium, according to Kirchhoff's Laws, this means:

- For $\mathbf{P}_G$

$$0 = p_{Gm} - p_{Dm} - v_m \sum_{n=1}^{NB} v_n [g_{m,n} cos(\theta_m - \theta_n) + b_{m,n} sin(\theta_m - \theta_n)] \tag{13}$$

- For $\mathbf{Q}_G$

$$0 = q_{Gm} + q_{Cm} - q_{Dm} - v_m \sum_{n=1}^{NB} v_n [g_{m,n} sin(\theta_m - \theta_n) - b_{m,n} cos(\theta_m - \theta_n)] \tag{14}$$

Note that the summation of the energy consumed by the network must be zero. Here, NB is the number of buses, p_{Gm}, q_{Gm} are the injected powers (real and reactive), p_{Dm}, q_{Dm} are the load powers (real and reactive), $g_{m,n}$, $b_{m,n}$ are the conductance and susceptance of the load presented between the nodes m, n. In practice, we should consider that few branches are connected to the node m. For this case, these functions are considered as $g(\mathbf{x}, \mathbf{u})$.

The dimension D depends on the scenario to be analyzed and is related to the size of the independent vector $\mathbf{u}$. The value of D can be found in Methodology Section VI, item 2. Also, the constraints can be found in detail in the Methodology Section.

IV. DESCRIPTION OF THE OBJECTIVE FUNCTION

The objective function is defined by:

$$f(x, u) = f_s(u), \tag{15}$$

and each $f_s(u)$ may be equal to the following functions found in the literature

- Minimize the MC, represented as: [17], [18], [19].

$$f_1(u) = \sum_{i=1}^{NG} a_i + b_i p_{Gi} + c_i (p_{Gi})^2 (\$/h) \tag{16}$$

- Minimize the total MC+VP, represented as: [17], [18], [19].

$$f_2(u) = \sum_{i=1}^{NG} (a_i + b_i p_{Gi} + c_i (p_{Gi})^2) + \hat{f}_2(x)(\$/h) \tag{17}$$

where

$$\hat{f}_2(x) = w \sum_{i=1}^{NL} |V_i - 1.0| (\$/h) \tag{18}$$

and V_i is the voltage magnitude. The difference with Eq. 16 is the inclusion of Eq. 18.

- Minimize the total cost function with V/P|POZ [11]:

$$f_3(u) = \sum_{i=1}^{NG} a_i + b_i p_{Gi} + c_i (p_{Gi})^2 + \ldots |d_i \times sin\left[e_i \times (p_i^{min} - p_{Gi})\right]| (\$/h) \tag{19}$$

- Minimize the total MC of a PWQC with multi-fuel sources, represented as: [17], [18], [19].

$$f_q(u) = \sum_{i=1}^{NG} a_{ik} + b_{ik} p_{Gi} + c_{ik} (p_{Gi})^2 (\$/h) \tag{20}$$

where k indicates how the power cost is divided into pieces and $P_{ik} \leq P_i \leq P_i^{max}$.

A. PENALTY FACTORS

Using the penalty factors eases the implementation of each nature-inspired optimization algorithm for this problem [18]. Without penalty factors in the fitness function, the validation becomes an unmanageable task, and more inner cycles are needed to solve the problem and satisfy the constraints. Mathematically, penalty factors are added and expressed in Eq. 21 as:

$$\begin{aligned} f_s^p(x,u) = f_s(u) &+ \lambda_P (p_{G1} - p_{G1}^{lim})^2 \\ &+ \ldots \lambda_V \sum_{j=1}^{NL} (v_{Lj} - v_{Lj}^{lim})^2 \\ &+ \ldots \lambda_Q \sum_{j=1}^{NG} (q_{Gj} - q_{Gj}^{lim})^2 \\ &+ \ldots \lambda_S \sum_{j=1}^{nl} (|s_{lj}| - s_{lj}^{max})^2 \end{aligned} \tag{21}$$

where $f_s(u)$ is the function to be evaluated and

$$x_j^{lim} = \begin{cases} x_j^{max}, & x_j > x_j^{max} \\ x_j^{min}, & x_j < x_j^{min} \\ x_j, & \text{otherwise.} \end{cases} \tag{22}$$

It is necessary to clarify that the penalty summations should not contain elements inside the limits, only those outside (greater than or lower than). That means NL, NG, and nl are displayed to show where those elements are taken to compute the summations. Thus, the value of x^{lim} should equal x to obtain a zero contribution to the summation. In practice, the corresponding additions do not consider these elements inside the limits. On the other hand, the elements to be penalized are those outside the algorithm's control. For the term shown in Eq. 23 ([11], [24])

$$\lambda_S \sum_{j=1}^{nl} (|s_{lj}| - s_{lj}^{max})^2 \tag{23}$$

where $s_j^{l,max}$ is determined as the maximum supported power in the given branch and $|s_j^l|$ is the maximum absolute power obtained in the line j when computing the flow in both directions for that line, where the maximum computed value is taken.

B. ADDITIONAL CONSIDERATIONS

This problem should be considered continuous because the evaluated functions are of this nature. Thus, the MC, VP, and V/P effects and the PWQC formulation are computed as continuous quantities.

V. DIFFERENTIAL EVOLUTION ALGORITHM

The DE algorithm was proposed by Storn and Price [40]. Its typical core is based on a weighted equation of differences expressed in Eq. 24 as:

$$m^i = u^{r1} + M(u^{r2} - u^{r3}) \tag{24}$$

To form m^i, three different individuals are selected from the population: u^{r1}, u^{r2}, u^{r3}, where they also are different to the individual reference Pop_i. The expression shown in Eq. 24 is known as DE/Rand/1. DE is performed in 5 steps: initialization, mutation, recombination, validation, and selection.

The initialization step creates a matrix denoted as population Pop, where vectors called individuals are stored. Each individual is of length D. Each individual is by itself a starting solution candidate for the treated problem. Np denotes the number of complete individuals/solutions.

The mutation operation helps control the solution candidates nearest to the global optimum by controlling the difference among the individuals. The mutation process is controlled by Eq. 24, where $u^{r1}, u^{r2}, u^{r3} \in \{1, \ldots, Np\}$. That means u^{r1}, u^{r2} and u^{r3} are three different random individuals from the population and not related to the current target vector u^i. Additionally, $M \in (0, 1)$ is the mutation constant and is treated as the scaling element of the equation. Thus, the mutant individual m^i is obtained. The recommended value for M is 0.8, which is used in this manuscript [41].

In the recombination step, the mutant individual m^i and the current target vector u^i create a new candidate vector t^i. The way to do this is by generating two random numbers, $rand \in [0, 1]$ and $Rnd \in \{1, .., D\}$. Then, $rand$ is compared to the recombination constant $Cr \in (0, 1)$ and Rnd is compared against the current component j to determine if the mutant element $m^{i,j}$ is stored in $t^{i,j}$:

$$t^{i,j} = \begin{cases} m^{i,j} & if\ rand \leq Cr\ or\ Rnd = j \\ & \forall j \in \{1, \ldots, D\} \\ u^{i,j} & otherwise\ . \end{cases} \tag{25}$$

The recommended value for Cr is 0.9, which is used in this manuscript [41].

The validation process is done for t^i, where each component $t^{i,j}$ is validated against the established constraints of the problem to be solved. If $t^{i,j}$ is outside its corresponding boundaries, $t^{i,j}$ is substituted by a new $t^{i,j}$ generated randomly but inside the respective boundaries.

Finally, the selection operator compares the fitness of the trial vector t^i and the fitness of the target vector u^i. At the end of the operation, a new individual is created, thus improving the computation of the fitness for the next generations. Eq. 26 summarizes this operation as

$$Pop_i = \begin{cases} t^i & if\ f_s^p(x, t^i) < f_s^p(x, u^i) \\ u^i & otherwise\ , \end{cases} \tag{26}$$

where pop_i is the new individual which results from the selection operation, taking the best individual between t^i and u^i according to their corresponding fitness output. That means if the new t^i cannot improve the objective function, it is rejected; otherwise, it is accepted and becomes the new individual of the population.

To obtain better individuals, the operations of recombination and selection are used. To remain near the global optimum, mutation and validation operations are applied to generate new individuals who preserve features of their corresponding ancestors. Depending on the conditions and parameters, DE can create new, better individuals in the population each time it iterates. This is done until a feasible solution is obtained. The final population is expected to stay near the global optimal solution to the problem. The more iterations, the more accurate the solution. These iterations are denoted as generations ($\hat{G}$) because a new population Pop is produced from the previous one.

Different ways of performing the recombination operation for DE are available. For instance, in Eq. 27, the variant DE/Best/1 is shown, where $r1$ is substituted with the *best* element among Pop:

$$m^i = u^{best} + M(u^{r1} - u^{r2}) \tag{27}$$

Lezama et al. [42] suggest using a random factor $randb \in [0, 1]$ to enhance the convergence of DE to reduce the stagnation and speed up the convergence. Then, Eq. 24 becomes Eq. 28 as:

$$m^i = u^{r1} + (randb)M(u^{r2} - u^{r3}). \tag{28}$$

and the rand variant for DE/Best/1 is expressed in Eq. 29 as:

$$m^i = u^{best} + (randb)M(u^{r2} - u^{r3}). \tag{29}$$

The pseudo-code of DE applied to OPF is shown in Algorithm 1, where *Fitness* stores the function evaluations with the penalty factors and *Outputs* stores the function evaluation without these penalty factors.

Algorithm 1 DE Applied to OPF

```
Input the control parameters for DE
Build initial population Pop
Evaluate fitness for each individual in Pop
Begin generations counter s = 1
for s = 1 to Ĝ do
    for i = 1 to Np do
        Generate random individuals.
        Do mutation m^i according to Eq. 24 (or another variant);
        Recombination to obtain t^i. Eq. 25;
        Validate t^i.
        Update t^i if needed;
        Solve t^i with Newton-Raphson (MATPOWER [43], [44]);
        Apply selection operator Eq. 26;
    end for
end for
Pop_best obtained with the lowest fitness.
return Pop_best, Fitness, Outputs
```

VI. METHODOLOGY

Supplementary information of the IEEE-30 and IEEE-57 networks is in the Appendix section.

The steps for analyzing the problem are: 1. Verify that each variable does not violate the upper and lower limits in a significant way; 2. Verify that Kirchhoff's Law tends to zero by solving the system with Newton-Raphson's Method. In summary, the general constraints and initial conditions for all the tested nature-inspired algorithms are listed as follows:

1) The population size is $Np = 100$.
2) The dimension D for the electric network IEEE-30 is $D = 24$, for the electric network IEEE-57 is $D = 33$ (the size of the vector $\mathbf{u}$).
3) Let $\lambda_P = 100$, $\lambda_V = 100000$, $\lambda_Q = 100$, $\lambda_S = 100$ [29]. For the IEEE-30, $\hat{G} = 500$; meanwhile for IEEE-57, $\hat{G} = 2500$. For $f_2^p(x, u)$, $w = 100$ [19].
4) For $f_2^p(x, u)$ and the electric network IEEE-57 ($f_{57}(u)$), each lambda is multiplied by a factor of $1,000,000$. For $f_1(u)$, $f_q(u)$ and $f_3(u)$, each lambda is left *as-is*.
5) Each individual of the population begins as $Pop_i = \mathbf{u}^i$, $\mathbf{u}^i = [\mathbf{P}_{i,G}\ \mathbf{V}_{i,G}\ \mathbf{Q}_{i,C}\ \mathbf{T}_i]$, $\mathbf{x}^i = [p_{i,G1}\ \mathbf{V}_{i,L}\ \mathbf{Q}_{i,G}\ \mathbf{S}_{i,l}]$ and $Pop_{initial} = Pop_1$.
6) The validation process is done for each component of $\mathbf{u}^i$, not for $\mathbf{x}^i$ that depends on the Newton-Raphson method. The components in $\mathbf{x}^i$ obtained with Newton-Raphson are left "as is", even if the constraints are surpassed because it is expected that the penalty factors can reduce these surpassed quantities when they are substituted in Eq. 21 until they vanish.
7) The penalty factors should help the fitness function to converge by including the appropriate constraints in Eq. 21. At the same time, these summations will vanish if the constraints are fulfilled when executing each generation. It is expected that the more generations, the more summations will vanish.
8) All the tests presented in this manuscript were launched 100 times to obtain each scenario's corresponding means, maximum and minimum values.

9) A successful trial is considered if and only if $f_s^p(x,u) - f_s(u) = 0$. Otherwise, the solution is not feasible because the penalty factors are not being mitigated/vanished.

In summary, the feasible solution is stored in $\mathbf{u}^i$ and the elements to be reduced in Eq. 21 are stored in $\mathbf{x}^i$. When $\mathbf{x}^i$ is evaluated, it is expected that such evaluation fits with the condition $f_s^p(x,u) - f_s(u) = 0$, where such a result means that all the elements stored in $\mathbf{x}^i$ fulfill the given constraints. Each best feasible solution $\mathbf{u}^i$ for each bio-inspired method is presented in Tables 5 and 7.

VII. RESULTS

A. SPECIFICATION OF THE CASES CONSIDERED

Using the notation in Table 2 and the equations described in Section IV, the cases to be considered are the following:

- Case 1. Cost optimization or MC (Eq. 16) [17], [18], [19].
- Case 2. Cost with voltage profile or MC+VP (Eq. 17) [17], [18], [19].
- Case 3. Cost with the inclusion of prohibited zones and valve point effects or V/P|POZ (Eq. 19) [11].
- Case 4. With multi-fuel sources and piecewise quadratic costs or PWQC (Eq. 20) [17], [18], [19].

All of the above cases are considered for the network IEEE-30, while for the IEEE-57 only the first case is considered. For the aforementioned scenarios and using DE, the four mutation operators were applied, where

DE $\rightarrowtail$ means to use Eq. 24.
DEAR $\rightarrowtail$ means to use Eq. 27.
DEAB $\rightarrowtail$ means to use Eq. 28.
DEABR $\rightarrowtail$ means to use Eq. 29.

For each tested algorithm, the best case is labeled by superscript z in the way $f_s^z(u)$. Also, the best results are highlighted with bold fonts for each algorithm. Moreover, four additional nature-inspired algorithms are also tested: PSO [6], TL [7], BBO [8], ABC [9]. We developed our own implementations for DE and TL. The rest of the nature-inspired algorithms are adaptations of the templates downloaded from www.yarpiz.com [45].

B. RESULTS OBTAINED FOR IEEE-30 NETWORK

For IEEE-30 [19], [31], two scenarios are considered. They are as follows:

- Scenario 1. Capacitors with value equal to zero ($C_{10} = 0$; $C_{24} = 0$). There are not coupling line capacitors. In practice, these values are modified in MATPOWER by rewriting them. These cases are denoted as $f_s(u)$.
- Scenario 2. Capacitors with their nominal value (found in MATPOWER as $C_{10} = 19.0$; $C_{24} = 4.3$, but converted to p.u as $C_{10} = 0.190$; $C_{24} = 0.043$, respectively). In practice, these values are left *as is* in MATPOWER. These cases are $f_{s,c}(u)$.

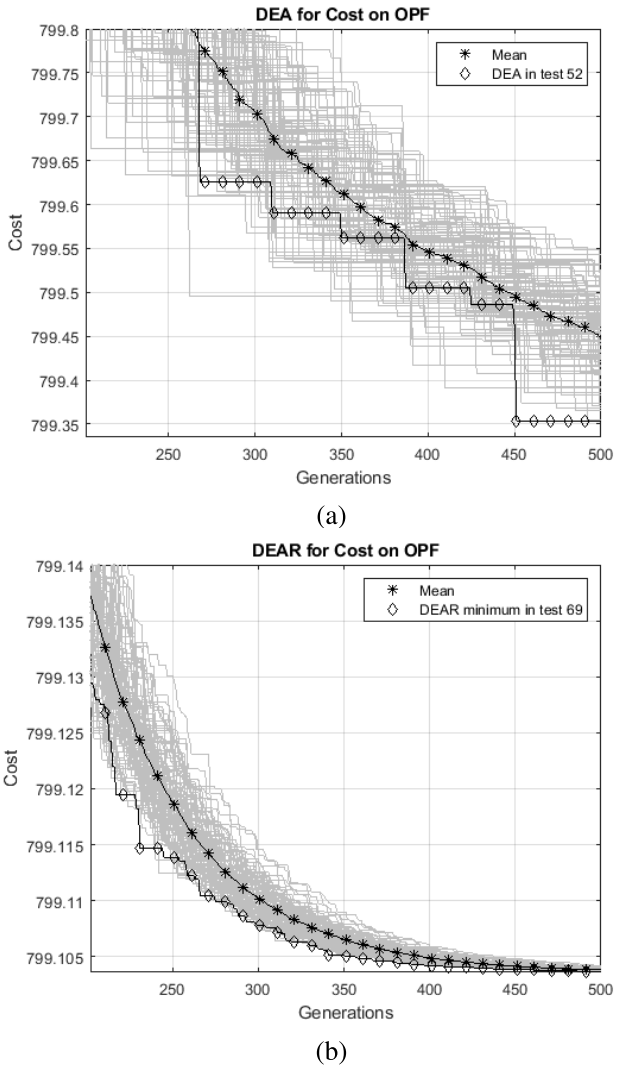

FIGURE 1. Set of curves for (a) DE and (b) DEAR applied to $f_1^p(x,u)$.

1) DE OPTIMIZATION

Fig. 1 shows the family of curves obtained for DE and DEAR and their corresponding means and minima values. 95 outputs were considered for DE, whereas the full set of outputs was included to compute the mean and the minimum for DEAR. This is done to discard those curves that do not converge, i.e., if they do not meet the condition $f_1^p(x,u) - f_1(u) = 0$. Only the last 200 generations are displayed for the sake of easy comparison, a practice extended to other analyzed nature-inspired techniques. Initially, it's evident that DE exhibits slower convergence and higher curve values compared to DEAR. In contrast, DEAR shows more focused curves as its set approaches the likely optimal solution. The mean for the set of 95 DE curves is $\hat{\mu} = 799.4484$. Meanwhile, the mean for 100 DEAR curves is $\hat{\mu} = 799.1038$. The minima values are obtained for $f_1^{p,52}(x,u)$ for DE and $f_1^{p,69}(x,u)$ for DEAR. The corresponding minima values are $\hat{m} = 799.3539$ and $\hat{m} = 799.1036$.

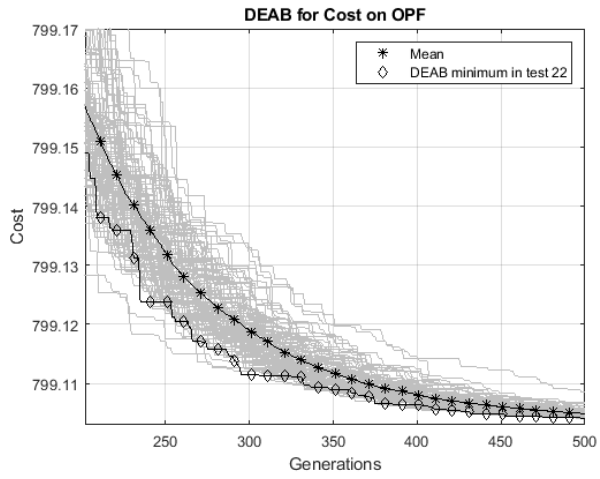

(a)

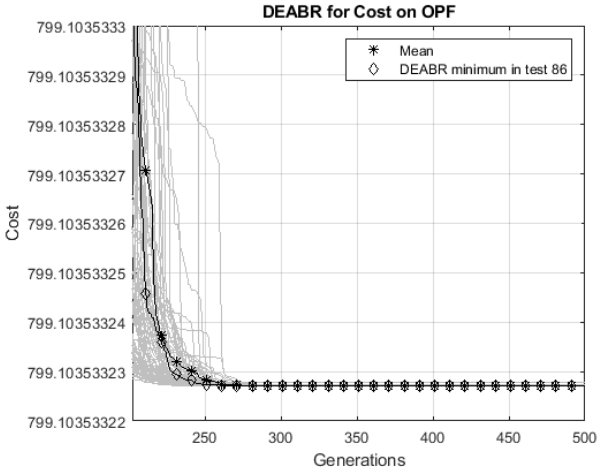

(b)

FIGURE 2. Set of curves for (a) DEAB and (b) DEABR applied to $f_1^p(x, u)$.

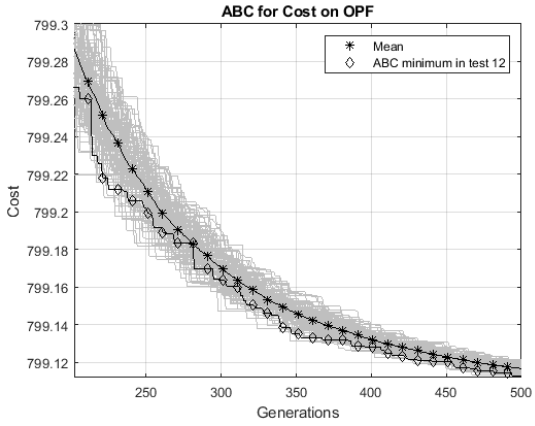

FIGURE 3. Set of curves for ABC applied to $f_1^p(x, u)$.

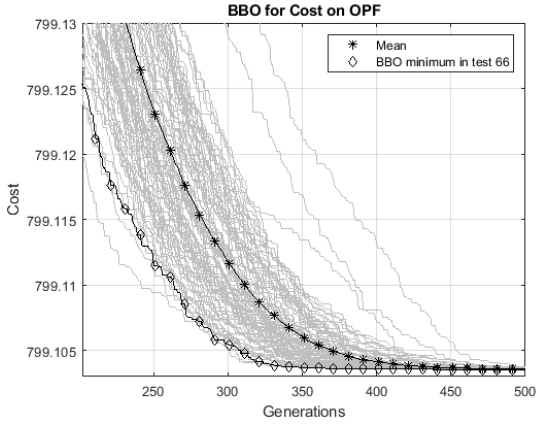

FIGURE 4. Set of curves for BBO applied to $f_1^p(x, u)$.

On the other hand, Fig. 2 shows the behavior of DEAB and DEABR. For these cases, the full set of tests (100) is considered to compute their respective means and minimum values. Compared to the cases presented in Fig. 1, DEAR and DEAB exhibit similar ranges and speeds in reaching the likely optimal solution. DEABR stands out as the fastest among all DE variants, quickly approaching the most likely optimal solution. The minima values are obtained for $f_1^{p,22}(x, u)$ for DEAB and $f_1^{p,86}(x, u)$ for DEABR. The corresponding minima values are $\hat{m} = 799.1040$ and $\hat{m} = 799.1035$.

The mean for the set of DEAB curves is $\hat{\mu} = 799.1049$, and the mean for the set of DEABR curves is $\hat{\mu} = 799.1035$, being the last one the best mean value among all the DE variants presented. Despite its fast behavior to reach the most likely optimal solution for $f_1^p(x, u)$.

2) ABC OPTIMIZATION

The ABC optimization algorithm was created by Karaboga et al. [9] and one of its applications for the OPF problem is provided by Adaryani et al. [23]. By using the Yarpiz Team platform [45], the main constant parameters to be configured for the BBO were: $a = 1$ (acceleration coefficient), the number of onlooker bees which is equivalent to the population, and $L = round(0.6 * D * Np)$ (abandonment limit parameter). Fig. 3 shows the set of curves obtained with ABC, with the corresponding mean and minimum curves. The curve with the minimum value is obtained in the trial $f_1^{p,12}(x, u)$ with $\hat{m} = 799.1128$. The mean of the ABC curve set is $\hat{\mu} = 799.1167$ and is greater than DEABR with a difference of 0.0132.

3) BBO

Simon proposed the BBO nature-inspired optimization [8] and one of its applications to OPF is provided by Bhattacharya et al. [28]. By using the Yarpiz Team platform [45], the main constant parameters to be configured for the BBO were: KeepRate=0.2, alpha=0.9, pMutation=0.1, sigma=0.2(varmax-varmin), where varmax and varmin depend on the given constraints. The parameters mu (emigration rate) and lambda (immigration rate) are determined by the population size (see Section VI for more

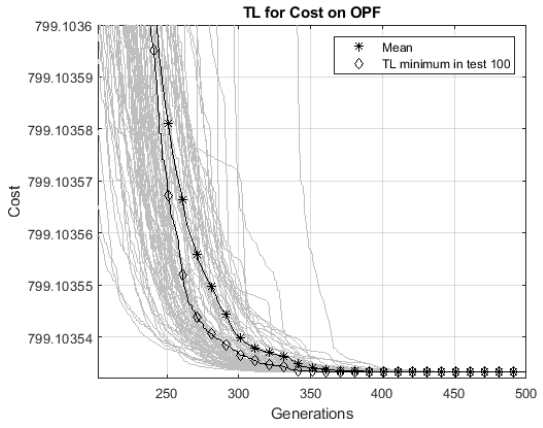

FIGURE 5. Set of curves for TL applied to $f_1^p(x, u)$.

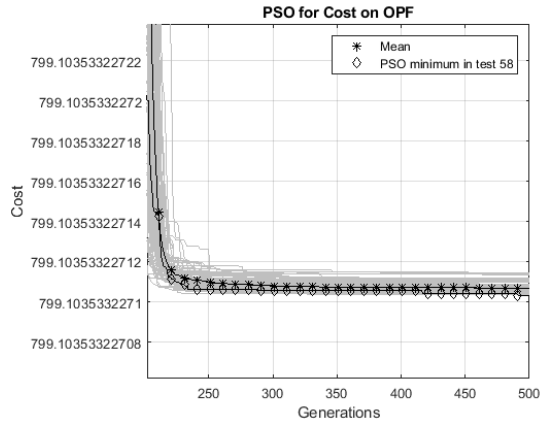

FIGURE 6. Set of curves for PSO applied to $f_1^p(x, u)$.

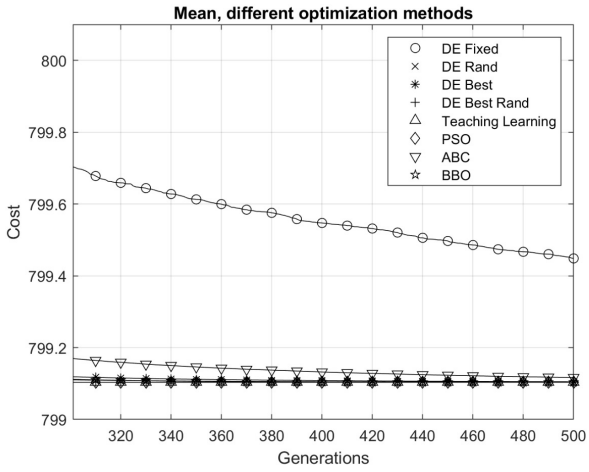

(a)

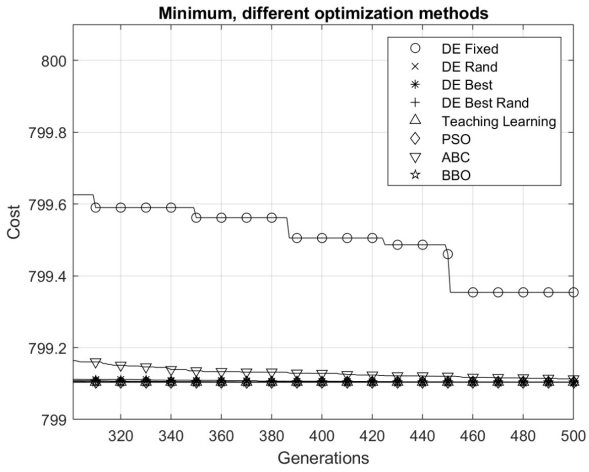

(b)

FIGURE 7. (a) Mean and (b) minimum values for the nature-inspired techniques tested in this manuscript for the function $f_1^p(x, u)$ on the IEEE-30 electric network.

details). Fig. 4 shows the set of curves obtained with BBO, with the corresponding mean and minimum curves. The curve with the minimum value is obtained in the trial $f_1^{p,66}(x, u)$ with $\hat{m} = 799.1035424118620$. The mean of the curve set of BBO is of $\hat{\mu} = 799.1035789326458$ and it is greater than the mean of DEABR $\hat{\mu} = 799.1035332271490$, where the difference is of $4.5705496746 \times 10^{-5}$

4) TL OPTIMIZATION

Rao proposed the TL optimization in [7], which is based on how an agent labeled as *Teacher* leads to improve the performance of those labeled *students*. The best performance is achieved by polishing the skills and ways of learning for each *student*. In any nature-inspired algorithm, the main idea is to improve the average that characterizes the performance of the *students* and then lead them to achieve an elitist performance. Thus, each *student* has the potential to reach the optimal solution when the number of *lessons* are taken. To do so, the best students are considered as *leaders* to help the other students improve their *notes*. For this case, the elitist number is left as $E = 10$. An example of this nature-inspired algorithm applied to the OPF is shown in [25].

Fig. 5 shows the set of curves obtained with PSO, with the corresponding mean and minimum curves. The curve with the minimum value is obtained in the trial $f_1^{p,100}(x, u)$ with $\hat{m} = 799.1035332271402$. For this case, extra digits are considered to compare and determine the best case between TL and DEABR. Being $\hat{\mu} = 799.1035332285726$ the mean for TL, it is seen that TL is worse than DEABR. Nevertheless, the difference is quite small, being only 1.423587×10^{-9}.

5) PSO

The PSO algorithm was developed by Shi et al. [6]. Its application to OPF has existed since its appearance, for instance, the work developed by Abido et al. [18]. It has continued through time, as shown by the application of this algorithm by Vo et al. [24]. By using the Yarpiz Team platform [45], the parameters to be configured for the PSO were: w=1 (inertia weight), wdamp=0.99 (inertia weight damping ratio), c_1=1.5 (personal learning coefficient), c_2=2.0 (global

TABLE 3. Running time data in seconds for $f_1^p(x,u)$ objective function.

Algorithm	N	Mean	SE Mean	StDev	Min	Q1	Median	Q3	Max
DE	98	318.59	0.0642	0.636	317.2	318.1	318.5	318.98	320.08
DEAR	100	320.65	0.103	1.03	318.89	319.88	320.41	321.3	323.18
DEAB	97	320.57	0.097	0.955	318.24	319.89	320.5	321.2	322.95
DEABR	98	321.76	0.0997	0.972	319.99	320.98	321.75	322.42	324.32
TL	98	751.3	0.632	6.16	737.16	746.73	751.86	754.98	766.49
PSO	98	327.46	0.0719	0.697	326.02	326.95	327.48	327.88	329.06
ABC	99	640.42	0.165	1.64	636.66	639.34	640.44	641.58	644.74
BBO	95	330.71	0.0501	0.488	329.51	330.4	330.69	331.1	331.84

TABLE 4. Mean ($\hat{\mu}$), minimum ($\hat{m}$) and maximum ($\hat{M}$) of the nature-inspired algorithms for the IEEE-30 electric network.

f_s	St.	DE	DEAR	DEAB	DEABR	TL	PSO	ABC	BBO
f_1	$\hat{\mu}$	799.4484	799.1038	799.1049	799.1035	799.1035	**799.1035**	799.1167	799.1035
	$\hat{M}$	799.5426	799.1042	799.1084	799.1035	799.1035	799.1035	799.1217	799.1037
	$\hat{m}$	799.3539	799.1036	799.1040	799.1035	799.1035	799.1035	799.1128	799.1035
$f_{1,c}$	$\hat{\mu}$	799.2559	799.0404	799.0404	Infeasible	Infeasible	**799.0399**	799.0474	799.0402
	$\hat{M}$	799.3455	799.0409	799.0413	Infeasible	Infeasible	799.0399	799.0510	799.0404
	$\hat{m}$	799.1646	799.0400	799.0401	Infeasible	Infeasible	799.0399	799.0446	799.0401
f_2	$\hat{\mu}$	818.5067	813.6586	**813.5555**	813.6240	813.6270	813.6131	814.8806	814.1350
	$\hat{M}$	819.8159	813.8758	813.7326	813.9759	814.6157	813.9418	815.2407	814.6989
	$\hat{m}$	816.8964	813.5187	813.4668	813.4377	813.4196	813.4543	814.4077	813.6267
$f_{2,c}$	$\hat{\mu}$	816.9666	812.9754	**812.8469**	812.8833	812.8754	812.8905	813.8005	813.2833
	$\hat{M}$	817.7827	813.1231	812.9567	813.3083	813.2869	813.4173	814.1481	813.8735
	$\hat{m}$	815.7076	812.8444	812.7775	812.7395	812.7508	812.7474	813.3848	812.8882
f_3	$\hat{\mu}$	835.0040	833.3268	833.3299	833.4229	**833.2775**	833.5420	834.2012	833.4139
	$\hat{M}$	835.4226	833.3752	833.4079	835.5585	833.4193	835.3219	834.8128	833.5534
	$\hat{m}$	834.2886	833.3003	833.2883	833.2495	833.2509	833.2818	833.8892	833.3158
$f_{3,c}$	$\hat{\mu}$	834.6004	833.2325	833.2200	**833.1864**	833.1981	833.3800	833.9605	833.2846
	$\hat{M}$	835.1149	833.2811	833.2578	833.2716	833.2529	835.2934	834.4935	833.3781
	$\hat{m}$	834.1416	833.2093	833.2030	833.1799	833.1813	833.1865	833.5926	833.2162
f_q	$\hat{\mu}$	646.7074	645.3877	**645.2005**	646.0128	645.3011	645.2035	647.5332	645.7662
	$\hat{M}$	647.2245	645.5719	645.2776	722.8389	646.9675	645.7112	648.0598	647.3181
	$\hat{m}$	646.0217	645.2750	645.1592	645.1225	645.1255	645.1232	646.9272	645.2636
$f_{q,c}$	$\hat{\mu}$	646.5115	645.2425	**645.0992**	645.1097	645.2987	645.2123	647.3312	645.3583
	$\hat{M}$	647.2378	645.3324	645.1419	645.1097	647.3994	645.6056	647.8764	645.8523
	$\hat{m}$	645.9579	645.1362	645.0814	645.1097	645.0712	645.0885	646.7464	645.1572

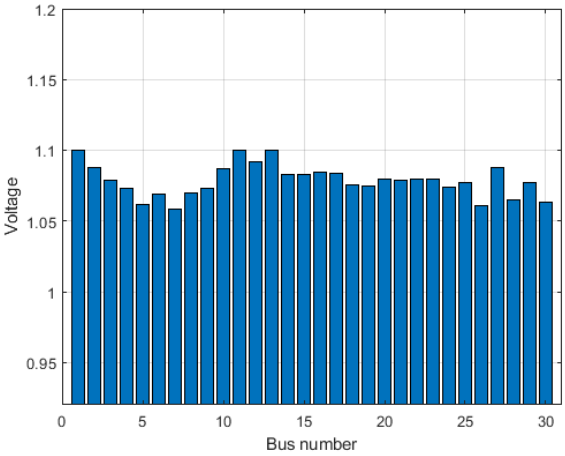

FIGURE 8. Voltage profile for $f_1^{58}(x)$ obtained with PSO.

learning coefficient), velmax=0.1*(varmax-varmin) (maximum velocity) and velmin=−velmax (minimum velocity), where varmax and varmin depend on the given constraints.

Fig. 6 shows the set of curves obtained with PSO, with the corresponding mean and minimum curves. The curve with the minimum value is obtained in the trial $f_1^{p,58}(x,u)$ with $\hat{m} = 799.1035332271034$. Being $\hat{\mu} = 799.1035332271067$ for PSO when compared to the mean of DEAB, PSO seems the best option among all the nature-inspired techniques here studied for $f_1^p(x,u)$, where the difference is of 4.2292×10^{-11} in favor of PSO.

6) FIRST APPROACH OF THE TESTED TECHNIQUES

Fig. 7 shows a summary of the curves representing the mean and the minimum for each nature-inspired technique tested in this manuscript for the IEEE-30 electric network. These curves were extracted from the previous figures to compare them straightforwardly. It is seen that DE and ABC present the greatest values among the tested nature-inspired techniques. On the other hand, the rest of the nature-inspired techniques present a similar behavior regarding how each method reaches the likely optimal solution. It is to be noticed that all the curves were computed with $f_1^p(x,u)$ and the computed mean for each one is considered for the cases

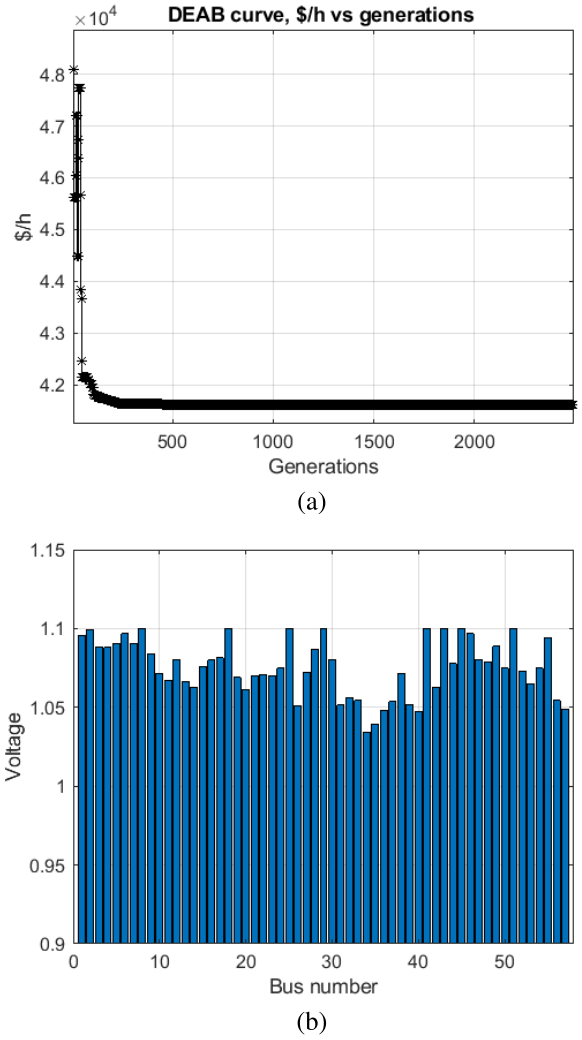

FIGURE 9. (a) Fitness curve and (b) voltage profile for $f_{57,1}^{49}(x)$ obtained with DEAB.

that fulfill $f_1^p(x,u) - f_1(u) = 0$. The best nature-inspired technique is chosen in the next subsection based on the lowest available mean for each analyzed case. As a first approach, the minimum curve from the set of curves showing the lowest available mean is considered the best solution.

We also conducted a thorough statistical analysis of the running times for each algorithm and objective function, and our findings revealed no significant evidence of sample biases or measurement errors. All simulations were executed on a dedicated MacBook Pro 2.3Ghz, 8-Core, Intel Core i9, 16GB of RAM computer, and running times were meticulously recorded. Due to manuscript length constraints, we are unable to provide detailed tables for each objective function. However, we have presented running time data obtained for objective function $f_1^p(x,u)$ as an illustrative example. In Table 3, you can find the specifics for the 100 running time data points obtained, with time recorded in seconds. The table indicates that the number of outliers is not substantial, and the maximum mean difference between data with and without outliers is 0.48 seconds. Subsequently, we provide descriptive statistics for each algorithm applied to the $f_1^p(x,u)$ objective function, highlighting that the maximum standard error for the mean is at most 0.462 seconds.

C. EXTENDED RESULTS FOR THE TREATED SCENARIOS

Table 4 shows the mean (μ), the maximum ($\hat{M}$) and the minimum ($\hat{m}$) values for DE and its variants. The lowest mean is considered the main parameter for choosing the best algorithm. At first sight, DEABR is not feasible for $f_{1,c}(u)$ because the function with penalty factors does not converge to the tested function, i.e., $f_{1,c}^p(x,u) - f_{1,c}(u) = 0$ is not fulfilled. This condition is critical to determine whether a nature-inspired technique is reliable for obtaining feasible sub-optimal solutions. Table 4 also shows the rest of the nature-inspired functions by evaluating their respective $\hat{\mu}$, $\hat{M}$ and $\hat{m}$. TL is also unfeasible for $f_{1,c}(u)$, contrasting to the feasibility of TL when applied to $f_1(u)$. For $f_{1,c}(u)$ and $f_1(u)$, PSO has the best mean. For $f_2(u)$, $f_{2,c}(u)$, $f_q(u)$ and $f_{q,c}(u)$, the best mean results were obtained with DEAB, meanwhile, the best mean for $f_3(u)$ is obtained with TL. Finally, by considering the mean, DEABR is the best option for solving $f_{3,c}(u)$.

By considering the results shown in Table 4 in terms of $\hat{\mu}$, Table 5 shows the best cases for each tested function, i.e., these cases with the minimum fitness taken from the algorithm that has the best mean. Then, PSO has the best performance for $f_1^{58}(u)$ and $f_{1,c}^{62}(u)$, while TL is the best for $f_3^{35}(u)$. DEAB generates the best results for $f_2^{90}(u)$, $f_q^{74}(u)$, $f_{2,c}^{83}(u)$ and $f_{q,c}^{39}(u)$. DEABR is the best for $f_{3,c}^{8}(u)$. At the same time, the values for each case in terms of $\hat{f}_2(u)$ are also included for all the presented cases. When $f_2(u)$ is computed, it is seen that the voltage profile $\hat{f}_2(u)$ is reduced when compared to $f_1(u)$ and $f_2(u)$.

Fig. 8 shows the voltage profile for the evaluation of $f_1^{58}(u)$ with PSO, which is the best case in this scenario (test 58 of 100 tests). The constraints are fulfilled because the minima values are above 0.95 and the maxima values are below or equal to 1.1. For these voltages that are firstly optimized, their corresponding results are shown in Table 5, second column. It is seen that all the voltage values are larger than 1.05, which means a large voltage profile, i.e., a big value for $\hat{f}_2^{58}(u) = 1.8348$. When $f_1^p(u)$ becomes $f_2^p(u)$, $\hat{f}_2(u)$ is reduced by having a value of $\hat{f}_2(u) = 0.0974$ (see the second column of Table 5). On the other hand, the corresponding cost curve is also shown. It is highlighted that there are two curves, $f_1^p(x,u)$ (fitness curve) and $f_1(u)$ (cost curve), where both are equivalent if $f_1^p(x,u) - f_1(u) = 0$. For this case, the cost curve ($f_1(u)$, from 1 to 500) is displayed in the corresponding chart.

D. IEEE-57 RESULTS

Information of IEEE-57 network is in the Appendix section. For this network, the shunt capacitances are placed in buses 18, 25, and 53, with the values 10, 5.9, 6.3, respectively.

TABLE 5. Best solution cases, IEEE-30 electric network. Scenarios 1 and 2.

Feature	f_1^{58} PSO	f_2^{90} DEAB	f_3^{35} TL	f_q^{74} DEAB	$f_{1,c}^{62}$ PSO	$f_{2,c}^{83}$ DEAB	$f_{3,c}^{8}$ DEABR	$f_{q,c}^{39}$ DEAB
P_1	177.1551	176.3708	194.4126	139.9993	177.1482	176.3409	194.3779	139.9993
P_2	48.7207	48.9627	44.9998	54.9986	48.7194	48.8680	44.9999	54.9986
P_5	21.3116	21.5188	20.6390	24.0822	21.3094	21.8538	20.5363	24.0746
P_8	20.9471	22.0800	11.2865	34.9931	20.9333	21.7065	11.4082	34.9643
P_{11}	11.9071	12.2073	10.0064	18.5589	11.9131	12.3928	10.0000	18.4557
P_{13}	12.0000	12.1266	12.0000	17.1635	12.0000	12.0941	12.0000	17.2847
V_2	1.1000	1.0414	1.0999	1.0999	1.0999	1.0406	1.0999	1.0999
V_5	1.0878	1.0243	1.0791	1.0900	1.0878	1.0241	1.0792	1.0891
V_2	1.0616	1.0127	1.0536	1.0630	1.0617	1.0128	1.0541	1.0650
V_8	1.0695	1.0027	1.0667	1.0754	1.0696	1.0026	1.0670	1.0753
V_{11}	1.1000	1.0714	1.0999	1.0994	1.0889	1.0166	1.0999	1.0964
V_{13}	1.0999	0.9879	1.0999	1.0996	1.0999	0.9869	1.0999	1.0999
T_{11}	1.0473	1.0957	1.0999	1.0319	1.0455	1.0330	0.9973	0.9873
T_{12}	0.9000	0.9008	0.9052	0.9176	0.9310	0.9966	1.0899	1.0328
T_{15}	0.9880	0.9382	1.0307	0.9798	0.9693	0.9408	1.0044	0.9726
T_{36}	0.9674	0.9683	0.9844	0.9683	0.9603	0.9791	0.9763	0.9639
Q_{10}	4.9999	4.8346	4.9941	4.9593	0.0000	3.1248	4.9902	2.6345
Q_{12}	4.9999	0.0686	4.9990	4.8563	4.9999	0.1592	4.9998	4.7910
Q_{15}	4.9999	4.9967	4.9977	4.3547	4.9999	4.9931	4.9978	4.6524
Q_{17}	4.9999	0.0529	4.9999	4.9590	5.0000	0.0095	4.9994	4.7255
Q_{20}	4.9999	4.9885	4.9933	4.4239	4.3892	4.9994	4.5754	4.6338
Q_{21}	4.9999	4.9655	4.9999	4.8172	4.9999	4.9999	4.9998	4.7206
Q_{23}	3.9006	4.9783	4.0641	3.6117	2.0094	3.9138	2.2551	1.8959
Q_{24}	4.9999	4.9772	4.9993	4.7623	3.6261	4.9936	3.8101	3.4374
Q_{29}	2.9298	2.5883	2.7856	3.0995	2.4614	3.4867	2.6090	2.2977
$f_s(u)$	799.1035	813.4668	833.2509	645.1592	799.0398	812.7775	833.1799	645.0814
$\hat{f}_2(u)$	1.8348	0.0974	1.4673	1.8891	2.0289	0.0903	1.7258	2.0530

TABLE 6. Mean ($\hat{\mu}$), minimum ($\hat{m}$) and maximum ($\hat{M}$) of the nature-inspired algorithms for the IEEE-57 electric network, $f_{57,1}(u)$.

St.	DE	DEAR	DEAB	DEABR
$\hat{\mu}$	41686.6808	41622.1580	**41621.1158**	41625.1285
$\hat{M}$	41711.2627	41632.1537	41621.5057	41653.3305
$\hat{m}$	41662.2086	41621.1700	41620.9833	41621.4271
	TL	PSO	ABC	BBO
$\hat{\mu}$	41649.0739	41661.7478	41697.9131	41666.2302
$\hat{M}$	41668.5801	41674.6299	41725.8364	41673.4025
$\hat{m}$	41638.2804	41645.9677	41678.5843	41644.0029

TABLE 7. Best solution case for the IEEE-57 electric network.

Feature	$f_{57,1}^{49}(u)$ DEAB	Feature	$f_{57,1}^{49}(u)$ DEAB
P_1	142.5979	T_{19}	0.9008
P_2	89.9905	T_{20}	1.0757
P_3	44.8806	T_{31}	1.0075
P_6	72.0373	T_{35}	0.9888
P_8	461.4800	T_{36}	0.9968
P_9	94.8710	T_{37}	1.0216
P_{12}	358.8124	T_{41}	0.9877
V_1	1.0958	T_{46}	0.9570
V_2	1.0992	T_{54}	0.9107
V_3	1.0882	T_{58}	0.9737
V_6	1.0967	T_{59}	0.9609
V_8	1.0999	T_{65}	0.9690
V_9	1.0841	T_{66}	0.9345
V_{12}	1.0804	T_{71}	0.9685
Q_{18}	1.7578	T_{73}	0.9954
Q_{25}	4.9980	T_{76}	0.9704
Q_{53}	4.9983	T_{80}	0.9861
$f_{57,1}(u)$	41620.9833		
$\hat{f}_2(u)$	3.6586		

These shunt capacitances were left unmodified to obtain the results presented. Table 5 shows the summary of the tested

TABLE 8. Success rate of each nature-inspired algorithm with 100 tests.

Cases	DE	DEAR	DEAB	DEABR
$f_1(u)$	95	100	100	100
$f_{1,c}(u)$	96	55	46	0
$f_2(u)$	100	100	100	93
$f_{2,c}(u)$	100	100	100	95
$f_3(u)$	95	100	100	100
$f_{3,c}(u)$	91	100	100	95
$f_q(u)$	88	99	100	100
$f_{q,c}(u)$	81	98	90	1
$f_{57,1}(u)$	100	98	98	59
Cases	TL	PSO	ABC	BBO
$f_1(u)$	100	100	100	100
$f_{1,c}(u)$	0	2	96	20
$f_2(u)$	97	99	100	100
$f_{2,c}(u)$	100	96	100	100
$f_3(u)$	100	100	98	100
$f_{3,c}(u)$	100	98	99	100
$f_q(u)$	98	100	91	100
$f_{q,c}(u)$	34	5	81	97
$f_{57,1}(u)$	79	63	100	98

nature-inspired techniques for the electric network IEEE-57, where the evaluation of the cost is denoted as $f_{57,1}(u)$. By considering the mean, the best technique is DEAB, with $\hat{\mu} = 41621.1158$, $\hat{M} = 41621.5057$ and $\hat{m} = 41620.9833$.

Table 6 shows the corresponding values for the best case, obtained with DEAB for $f_{57,1}^{49}(u)$. It is highlighted that $f_{57,1}^{p,49}(x,u) - f_{57,1}^{49}(u) = 0$ i.e. the penalized function is equal to the evaluated objective function. The cost is $f_1^{49}(u) = 41620.9833$. With the voltages computed for this network, the voltage profile $\hat{f}_2(u)$ is computed as 3.6586.

Fig. 9 shows the output for the evaluation of $f_{57,1}^{49}(u)$ with DEAB (test 49 of 100 tests). It is verified that the

TABLE 9. Score ranking for ($\hat{\mu}$), minimum ($\hat{m}$) and maximum ($\hat{M}$) for all the tested objective functions and nature-inspired algorithms.

f_s	St.	DE	DEAR	**DEAB**	DEABR	TL	PSO	ABC	BBO
f_1	$\hat{\mu}$	8	5	6	2	3	1	7	4
	$\hat{M}$	8	5	6	2	3	1	7	4
	$\hat{m}$	8	5	6	2	3	1	7	4
$f_{1,c}$	$\hat{\mu}$	6	3	4	8	8	1	5	2
	$\hat{M}$	6	3	4	8	8	1	5	2
	$\hat{m}$	6	2	4	8	8	1	5	3
f_2	$\hat{\mu}$	8	5	1	3	4	2	7	6
	$\hat{M}$	8	2	1	4	5	3	7	6
	$\hat{m}$	8	5	4	2	1	3	7	6
$f_{2,c}$	$\hat{\mu}$	8	5	1	3	2	4	7	6
	$\hat{M}$	8	2	1	4	3	5	7	6
	$\hat{m}$	8	5	4	1	3	2	7	6
f_3	$\hat{\mu}$	8	2	3	5	1	6	7	4
	$\hat{M}$	7	1	2	8	3	6	5	4
	$\hat{m}$	8	5	4	1	2	3	7	6
$f_{3,c}$	$\hat{\mu}$	8	4	3	1	2	6	7	5
	$\hat{M}$	7	4	2	3	1	8	6	5
	$\hat{m}$	8	5	4	1	2	3	7	6
f_q	$\hat{\mu}$	7	4	1	6	3	2	8	5
	$\hat{M}$	5	2	1	8	4	3	7	6
	$\hat{m}$	7	6	4	1	3	2	8	5
$f_{q,c}$	$\hat{\mu}$	7	4	1	2	5	3	8	6
	$\hat{M}$	6	3	2	1	7	4	8	5
	$\hat{m}$	7	5	2	4	1	3	8	6
$f_{57,1}$	$\hat{\mu}$	7	2	1	3	4	5	8	6
	$\hat{M}$	7	2	1	3	4	6	8	5
	$\hat{m}$	7	2	1	3	4	6	8	5
Score		196	98	**74**	97	97	91	188	134

corresponding voltage profile is inside the given constraints and is consistent with those shown in Table 7. It is expected that the voltage profile can have a big value ($\hat{f}_2(u) = 3.6586$). Additionally, the corresponding cost curve $f_{57,1}^{49}(u)$ is also shown. Compared to the curve shown for the electric network IEEE-30, there is a *jump* behavior for the initial generations, which means that $f_{57,1}^{p,49}(x,u) - f_{57,1}^{49}(u) \neq 0$ for those generations. At the end of execution of DEAB, $f_{57,1}^{p,49}(x,u)$ (fitness curve) and $f_{57,1}^{49}(u)$ (cost curve) are equivalent ($f_{57,1}^{p,49}(x,u) - f_{57,1}^{49}(u) = 0$). The curve (from 1 to 2500) is displayed in the corresponding chart for this case. The reason to execute each nature-inspired algorithm 2500 generations for this network is to discard the *jumping* behavior. As the number of conditions to fulfill increases, so does the number of generations needed to obtain an accurate behavior to check if the algorithm to be evaluated is reaching the likely optimal solution.

VIII. DISCUSSION AND COMPARISONS

Reproducing all the aforementioned algorithms is done to determine their advantages and disadvantages. Also, to study how small differences lead to very different outputs and behaviors in the results. Table 8 shows the success rate of each nature-inspired algorithm on each scenario, where 100 tests were performed to determine if each nature-inspired method can obtain $f_s^p(x,u) - f_s(u) = 0$ i.e. if the penalty factors vanish. If so, the instance is considered valid; Otherwise, it is discarded. As established throughout this manuscript, the initial conditions are the same for all tested nature-inspired algorithms, where only proper specific initial configurations (recombination and network parameters) were configured differently.

For $f_1(u)$, DE had 5 failed tests, and the rest of the nature-inspired algorithms have a fully successful performance. Nevertheless, when the capacitors C_{10} and C_{24} ($f_{1,c}(u)$) are left in their nominal values, there are significant degradation performances for DEAR, DEAB, DEABR, TL, PSO and BBO, where the rate of success is below 70%. DEABR and TL have the worst performances, with zero successful tests when considered all together. PSO also has a very low success rate (2 among 100).

For $f_2(u)$, all nature-inspired algorithms have a success rate higher than 90%, meanwhile when the capacitors C_{10} and C_{24} ($f_{2,c}(u)$) are left in their nominal values, DEABR and PSO present no full successful performance (95% and 96%, respectively). For the scenario with the use of the multi-fuel sources (quadratic case, $f_q(u)$), DEA has the lowest success rate; meanwhile, DEAB, DEABR, PSO and BBO have full success rates. In contrast, by leaving the capacitors without modification i.e. with original values ($f_{q,c}(u)$), DEABR and PSO have highly degraded performances with 1 and 5 successful tests, respectively. Meanwhile, the best algorithm for this case is DEAR, with 98 of 100 successful trials. Finally, for the largest case, $f_{57,1}(u)$ DEABR and PSO have the worst performances with 59% and 63%, respectively. The full success rate is obtained with DEA and ABC.

The results presented in Table 8 indicate that a small change inside the same network (for this case, IEEE-30 when comparing Scenario 1 and Scenario 2, both described in Subsection VII-B) will lead to contrasting performances. For instance, the algorithms TL, PSO, and DEABR have a

good performance for Scenario 1, where they have 100/100 successful tests each one; meanwhile, for Scenario 2, their performance was degraded (2 of 100 for all of them). The aforementioned approaches were made because, in the literature, similar networks with small differences are often compared, or solutions considered *feasible* are established as the best ones without completely fulfilling all the constraints at all (i.e., an inaccurate penalty factor computing). In [33], the authors cite several unfeasible solutions reported as feasible. For these reasons, we do not present a comparison of our results to those of other works.

On the other hand, Table 9 shows how to rank each nature-inspired algorithm by applying the methodology followed by Castañón et al. [10]. The lowest rank (1) is assigned to that nature-inspired algorithm with the lowest fitness in terms of the mean ($\hat{\mu}$), the maximum ($\hat{M}$) and the minimum ($\hat{m}$), and so on (from 1 to 8) to the rest of the nature-inspired algorithms. The final score is obtained in the last row by doing a summation of the obtained scores for each algorithm applied on each objective function for each feature ($\hat{\mu}$,$\hat{M}$ and $\hat{m}$), where it is seen that DEAB has the lowest score (74). Nonetheless, by considering the success rate shown in Table 8, DEAB does not have good behavior when it is applied to $f_{1,c}(u)$, but still acceptable (46 of 100 trials). DE and ABC have the largest scores to be considered successful algorithms. Thus, DEAB has an acceptable compromise between a good success rate and good lower fitness values. A clarification note must be made, for $f_1(x, u)$, the largest value 8 was assigned to DEABR and TL because the penalty terms do not vanish i.e. their solutions are unfeasible as shown in Table 4.

IX. CONCLUSION AND FUTURE IMPROVEMENTS

In this work, we applied well-known nature-inspired algorithms to solve the OPF, i.e., DE and some of its variants, TL, PSO, ABC, and BBO, where the electric networks IEEE-30 and IEEE-57 were analyzed with their corresponding constraints and initial conditions. Only the initial configurations were different on each nature-inspired algorithm where appropriate. This way, we obtain several solutions regarding cost, voltage deviation, and valve point effect with prohibited zones and multi-fuel sources (quadratic case). Having these results available, an analysis of the success rate of penalty-vanishing terms and a ranking process was done to determine the best nature-inspired algorithm.

A small change in the network for those *constant* initial conditions for the electric network IEEE-30 will lead to contrasting behavior of each nature-inspired algorithm, as discussed in the previous section, where the match between the real fitness function and its penalized version is entirely affected, and reflected in the success rate of penalty-vanishing terms. On the other hand, it was necessary to establish a ranking process to determine which of the tested nature-inspired algorithms presents the best compromise in terms of its mean, maximum, and minimum fitness values with different objective functions. Combining the aforementioned criteria (ranking process and success rate of convergence), DEAB has the most acceptable compromise between the lowest successful behavior (74) and good lower fitness values among all the tested nature-inspired algorithms for all the tested objective functions.

As the next goal, different variants of the network IEEE-30 will be tested with other nature-inspired algorithms, including emissions and other features combined with power sources coming from renewable energies (wind, etc.). New hybrid metaheuristic algorithms named cross entropy (CE), covariance matrix adaption evolutionary strategy (CMAES) [46] and DE variants such as success history based adaptive differential evolution (SHADE) [47], JADE [34], and Hybrid-adaptive DE (HyDE) [48], [49] can be tested for this problem. The approach presented will be extended to include issues related to placement of controllers in a network as shown in [50], [51], [52], and [53], intelligent control of network variables as shown in [54], [55], and [56], minimization losses/costs with graph-oriented analysis [57], [58], classification of network variables depending on security behavior [59] and novel techniques to solve PF efficiently rather than the classical techniques [60], [61], [62].

APPENDIX

This Appendix provides information of networks IEEE-30 and IEEE-57 used in this analysis. It is important to mention that the parameters of both electric networks were loaded and configured with MATPOWER 6.0 according to [43] and [44].[1]

A. IEEE-30

This network is formed by $NB = 30$ buses and $nl = 41$ lines. There is one slack bus, five PV buses (with power injection), and the rest are PQ buses (load buses). This work implements the version analyzed by Abou et al. [17]. The schematic is shown in Fig. 10. The parameters are as follows:

- The impedance and the bus admittance can be found in [17], where these parameters are configured in MATPOWER [43], [44]. The power limits on each line are divided as shown in Table 10 and are taken from [24]. The operation limits of transformers ($\mathbf{T}_N$) are $0.9 \leq t_m \leq 1.1$, being the initial conditions on the given buses as taken from [17]: line 11, 1.078,0; line 12, 1.069,0; line 15, 1.032,0 and line 36, 1.068,0. The corresponding angles are in degrees, and such angles remain with zero value throughout the bio-inspired algorithms.
- The coefficient costs are shown in Table 11.
  The reader should be aware that the last three columns in Table 11 are related to Eq. 19, where the last column shows the range of prohibited zones, i.e., those values that the power of the respective source must not have.
  For the multi-fuel case, sources G_1 and G_2 with the values given in Table 12, where the first two lines are for G_1 and the last two lines are for G_2.

[1] Available for download in http://www.pserc.cornell.edu/matpower/

TABLE 10. Power limit parameters for IEEE-30 network, taken from Vo et al. [24].

l_j	1	2	3	4	5	6	7	8	9	10	11	12	13	14	15	16	17	18	19	20	21
s_{lj}^{max}	130	130	65	130	130	65	90	70	130	32	65	32	65	65	65	65	32	32	32	16	16
l_j	22	23	24	25	26	27	28	29	30	31	32	33	34	35	36	37	38	39	40	41	-
S_{lj}^{max}	16	16	32	32	32	32	32	32	16	16	16	16	16	16	65	16	16	16	32	32	-

TABLE 11. Coefficient costs for IEEE-30 network, taken from Abou et al. [17] and Niknam et al. [11].

G	a	b	c	d	e	Prohibited zones
1	0.00	2.00	0.00375	18	0.037	[55-66], [80-120]
2	0.00	1.75	0.01750	16	0.038	[21-24], [45-55]
5	0.00	1.00	0.06250	14	0.04	[30-36]
8	0.00	3.25	0.00834	12	0.045	[25-30]
11	0.00	3.00	0.02500	13	0.042	[25-28]
13	0.00	3.00	0.02500	13.5	0.041	[24-30]

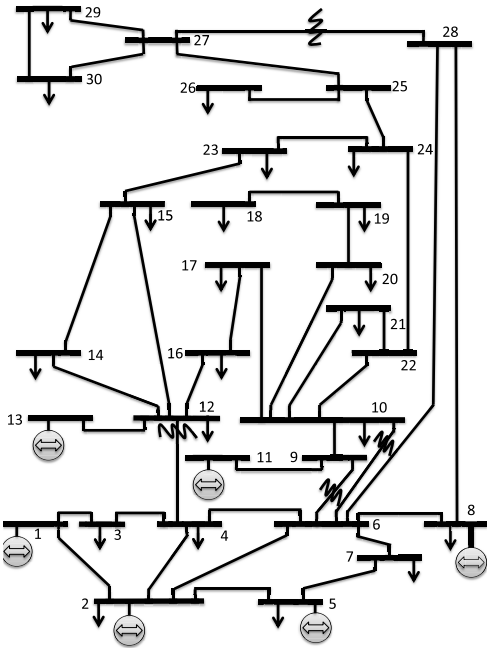

FIGURE 10. IEEE-30 network found in [17].

TABLE 12. Coefficient costs and power parameters for IEEE-30 network applied to the quadratic case, taken from Abou et al. [17].

P_{low}	P_{high}	a	b	c
50	140	55	0.70	0.0050
140	200	40	0.30	0.0100
20	55	82.5	1.05	0.0075
55	80	80	0.60	0.0200

- The initial voltages are 1.05, 1.04, 1.01, 1.01, 1.05, 1.05 for the buses 1, 2, 5, 8, 11, 13, being the first one the slack bus. The voltage limits for the generators ($\mathbf{V}_G$) are $0.95 \leq v_m \leq 1.10$. The values for the voltage limits on each load line are the same.
  Additionally, the real power limit values $\mathbf{P}_G$ for the buses 1, 2, 5, 8, 11, 13 are 50, 20, 15, 10, 10, 12 as the minimum and 200, 80, 50, 35, 30, 40 as the maximum, respectively. Meanwhile, the reactive power limit values $\mathbf{Q}_G$ for the buses 1, 2, 5, 8, 11, 13 are -20, -20, -15, -15, -10, -15 as the minimum and 200, 100, 80, 60, 50, 60 as the maximum, respectively. These values are included in Table 13. The rest of power loads on each bus are given in Table 14.
- The reactive powers stored in $\mathbf{Q}_c$ for the shunts are delimited by $0.0 \leq q_m \leq 5.0$ (not in p.u.). These shunts are set for places 10, 12, 15, 17, 20, 21, 23, 24, 29.

TABLE 13. Power parameter limits and initial voltages for IEEE-30 network, taken from Abou et al. [17].

Bus	V	P_G^{max}	Q_G^{max}	P_G^{min}	Q_G^{min}
1	1.05	200	200	50	-20
2	1.04	80	100	20	-20
5	1.01	50	80	15	-15
8	1.01	35	60	10	-15
11	1.05	30	50	10	-10
13	1.05	40	60	12	-15

TABLE 14. Load power parameters for IEEE-30 network, taken from Abou et al. [17].

Bus	P	Q	Bus	P	Q
1	0.000	0.000	16	0.035	0.018
2	0.217	0.127	17	0.090	0.058
3	0.024	0.012	18	0.032	0.009
4	0.076	0.016	19	0.095	0.034
5	0.942	0.190	20	0.022	0.007
6	0.000	0.000	21	0.175	0.112
7	0.228	0.109	22	0.000	0.000
8	0.300	0.300	23	0.032	0.016
9	0.000	0.000	24	0.087	0.067
10	0.058	0.020	25	0.000	0.000
11	0.000	0.000	26	0.035	0.023
12	0.112	0.075	27	0.000	0.000
13	0.000	0.000	28	0.000	0.000
14	0.062	0.016	29	0.024	0.009
15	0.082	0.025	30	0.106	0.019

B. IEEE-57

This network is formed by $NB = 57$ buses and $nl = 80$ lines. There is one slack bus, six PV buses, and the rest are PQ buses. In this work, the version analyzed is implemented in [24] and based on the configuration found in MATPOWER [43], [44]. For the sake of simplicity, the schematic of this network is omitted. Nevertheless, the parameters of this electric network are provided as follows:

- The impedance and the bus admittance can be obtained from MATPOWER [43], [44]. The operation limits of transformers ($\mathbf{T}_N$) are $0.9 \leq t_m \leq 1.1$. The power limit on each line was retrieved from [24] as shown in Table 15
- The coefficient costs are shown in Table 16.
- The initial voltages are 1.04, 1.01, 0.985, 0.980, 1.005, 0.980, and 1.015 for the buses 1, 2, 3, 6, 8, 9, 12, being

TABLE 15. Power limits for IEEE-57 network, taken from Vo et al. [24].

l_j	1	2	3	4	5	6	7	8	9	10	11	12	13	14	15	16-80
S_{lj}^{max}	150	85	100	100	50	40	100	200	50	50	50	50	50	100	200	100

TABLE 16. Coefficient costs for IEEE-57 network, taken from Vo et al. [24].

G	a	b	c
1	0.00	20	0.077579519
2	0.00	40	0.01
3	0.00	20	0.25
6	0.00	40	0.01
8	0.00	20	0.0222222222
9	0.00	40	0.01
12	0.00	20	0.0322580645

TABLE 17. Power limit parameters and initial voltages for IEEE-57 network, taken from Vo et al. [24].

Bus	V	P_G^{max}	Q_G^{max}	P_G^{min}	Q_G^{min}
1	1.040	575.88	200	0	-140
2	1.010	100	50	0	-17
3	0.985	140	60	0	-10
6	0.980	100	25	0	-8
8	1.005	550	200	0	-140
9	0.980	100	9	0	-3
12	1.015	410	155	0	-150

TABLE 18. Load power parameters for IEEE-57 network, taken from Vo et al. [24].

Bus	P	Q	Bus	P	Q
1	0.55	0.17	30	0.036	0.018
2	0.03	0.88	31	0.058	0.029
3	0.41	0.21	32	0.016	0.008
4	0.00	0.00	33	0.038	0.019
5	0.13	0.04	34	0.00	0.00
6	0.75	0.02	35	0.06	0.03
7	0.00	0.00	36	0.00	0.00
8	1.50	0.22	37	0.00	0.00
9	1.21	0.26	38	0.14	0.07
10	0.05	0.02	39	0.00	0.00
11	0.00	0.00	40	0.00	0.00
12	3.77	0.24	41	0.063	0.03
13	0.18	0.023	42	0.071	0.044
14	0.105	0.053	43	0.02	0.01
15	0.22	0.05	44	0.12	0.018
16	0.43	0.03	45	0.00	0.00
17	0.42	0.08	46	0.00	0.00
18	0.272	0.098	47	0.297	0.116
19	0.033	0.006	48	0.00	0.00
20	0.023	0.01	49	0.18	0.085
21	0.00	0.00	50	0.21	0.105
22	0.00	0.00	51	0.18	0.053
23	0.063	0.021	52	0.049	0.022
24	0.00	0.00	53	0.20	0.10
25	0.063	0.032	54	0.041	0.014
26	0.00	0.00	55	0.068	0.034
27	0.093	0.005	56	0.076	0.022
28	0.046	0.023	57	0.067	0.02
29	0.17	0.026	-	-	-

the first one the slack bus. The voltage limits for the generators ($\mathbf{V}_G$) are $0.90 \leq v_m \leq 1.10$. The values for the voltage limits on each load line are the same.

Additionally, the real power limit values $\mathbf{P}_G$ for the buses 1, 2, 3, 6, 8, 9, and 12 are 575.88, 100, 140, 100, 550, 100, and 410 as the maximum and 0 as the minimum for all the places, respectively. Meanwhile, the reactive power limit values $\mathbf{Q}_G$ for the same places are -140, -17, -10, -8, -140, -3 and -150 as the minimum and 200, 50, 60, 25, 200, 9 and 155 as the maximum, respectively. These values are shown in Table 17. The power loads on each bus are given in Table 18.

- The reactive powers stored in $\mathbf{Q}_c$ are delimited by $0.0 \leq q_m \leq 5.0$ (not in p.u.). These shunts are set for buses 18, 25, and 53.

ACKNOWLEDGMENT

Fernando Lezama would like to thank the work facilities and equipment provided by GECAD Research Center (UIDB/00760/2020), DOI:10.54499/UIDB/00760/2020 to the Project Team.

REFERENCES

[1] C.-M. Huang, H.-T. Yang, and C.-L. Huang, "Bi-objective power dispatch using fuzzy satisfaction-maximizing decision approach," *IEEE Trans. Power Syst.*, vol. 12, no. 4, pp. 1715–1721, Nov. 1997.

[2] K. H. Abdul-Rahman and S. M. Shahidehpour, "A fuzzy-based optimal reactive power control," *IEEE Trans. Power Syst.*, vol. 8, no. 2, pp. 662–670, May 1993.

[3] J. Nanda, "Economic emission load dispatch with line flow constraints using a classical technique," *IEE Proc. Gener., Transmiss. Distrib.*, vol. 141, no. 1, pp. 1–10, 1994.

[4] L. L. Lai, J. T. Ma, R. Yokoyama, and M. Zhao, "Improved genetic algorithms for optimal power flow under both normal and contingent operation states," *Int. J. Electr. Power Energy Syst.*, vol. 19, no. 5, pp. 287–292, Jun. 1997.

[5] J. K. Skolfield and A. R. Escobedo, "Operations research in optimal power flow: A guide to recent and emerging methodologies and applications," *Eur. J. Oper. Res.*, vol. 300, no. 2, pp. 387–404, Jul. 2022.

[6] Y. Shi, "Particle swarm optimization: Developments, applications and resources," in *Proc. Congr. Evol. Comput.*, Aug. 2001, pp. 81–86.

[7] R. V. Rao, V. J. Savsani, and D. P. Vakharia, "Teaching-learning-based optimization: A novel method for constrained mechanical design optimization problems," *Comput.-Aided Design*, vol. 43, no. 3, pp. 303–315, Mar. 2011.

[8] D. Simon, "Biogeography-based optimization," *IEEE Trans. Evol. Comput.*, vol. 12, no. 6, pp. 702–713, Dec. 2008.

[9] D. Karaboga and B. Basturk, "A powerful and efficient algorithm for numerical function optimization: Artificial bee colony (ABC) algorithm," *J. Global Optim.*, vol. 39, no. 3, pp. 459–471, Oct. 2007.

[10] G. Castañón, G. Campuzano, and O. Tonguz, "High reliability and availability in radio over fiber networks," *J. Opt. Netw.*, vol. 7, no. 6, pp. 603–616, 2008.

[11] T. Niknam, M. R. Narimani, and R. Azizipanah-Abarghooee, "A new hybrid algorithm for optimal power flow considering prohibited zones and valve point effect," *Energy Convers. Manage.*, vol. 58, pp. 197–206, Jun. 2012.

[12] M. S. Osman, M. A. Abo-Sinna, and A. A. Mousa, "A solution to the optimal power flow using genetic algorithm," *Appl. Math. Comput.*, vol. 155, no. 2, pp. 391–405, Aug. 2004.

[13] C. A. Roa-Sepulveda and B. J. Pavez-Lazo, "A solution to the optimal power flow using simulated annealing," *Int. J. Electr. Power Energy Syst.*, vol. 25, no. 1, pp. 47–57, Jan. 2003.

[14] R. E. Perez-Guerrero and J. R. Cedefio-Maldonado, "Differential evolution based economic environmental power dispatch," in *Proc. 37th Annu. North Amer. Power Symp.*, Dec. 2005, pp. 191–197.

[15] G. Y. Yang, Z. Y. Dong, and K. P. Wong, "A modified differential evolution algorithm with fitness sharing for power system planning," *IEEE Trans. Power Syst.*, vol. 23, no. 2, pp. 514–522, May 2008.

[16] N. Noman and H. Iba, "Differential evolution for economic load dispatch problems," *Electr. Power Syst. Res.*, vol. 78, no. 8, pp. 1322–1331, Aug. 2008.

[17] A. A. Abou El Ela, M. A. Abido, and S. R. Spea, "Optimal power flow using differential evolution algorithm," *Electr. Eng., Arch. Elektrotechnik*, vol. 91, no. 2, pp. 69–78, 2009.

[18] M. A. Abido, "Optimal power flow using particle swarm optimization," *Int. J. Electr. Power Energy Syst.*, vol. 24, no. 7, pp. 563–571, Oct. 2002.

[19] A. A. A. E. Ela, M. A. Abido, and S. R. Spea, "Differential evolution algorithm for optimal reactive power dispatch," *Electr. Power Syst. Res.*, vol. 81, no. 2, pp. 458–464, Feb. 2011.

[20] N. Amjady and H. Sharifzadeh, "Security constrained optimal power flow considering detailed generator model by a new robust differential evolution algorithm," *Electr. Power Syst. Res.*, vol. 81, no. 2, pp. 740–749, Feb. 2011.

[21] S. Sivasubramani and K. S. Swarup, "Sequential quadratic programming based differential evolution algorithm for optimal power flow problem," *IET Gener., Transmiss. Distrib.*, vol. 5, no. 11, pp. 1149–1154, 2011.

[22] T. Niknam, M. R. Narimani, J. Aghaei, and R. Azizipanah-Abarghooee, "Improved particle swarm optimisation for multi-objective optimal power flow considering the cost, loss, emission and voltage stability index," *IET Gener., Transmiss. Distrib.*, vol. 6, no. 6, pp. 515–527, 2012.

[23] M. R. Adaryani and A. Karami, "Artificial bee colony algorithm for solving multi-objective optimal power flow problem," *Int. J. Electr. Power Energy Syst.*, vol. 53, pp. 219–230, Dec. 2013.

[24] D. N. Vo and P. Schegner, "An improved particle swarm optimization for optimal power flow," in *Meta-Heuristics Optimization Algorithms in Engineering, Business, Economics, and Finance*. Hershey, PA, USA: IGI Global, 2013, pp. 1–40.

[25] H. R. E. H. Bouchekara, M. A. Abido, and M. Boucherma, "Optimal power flow using teaching-learning-based optimization technique," *Electr. Power Syst. Res.*, vol. 114, pp. 49–59, Sep. 2014.

[26] M. Ghasemi, M. M. Ghanbarian, S. Ghavidel, S. Rahmani, and E. M. Moghaddam, "Modified teaching learning algorithm and double differential evolution algorithm for optimal reactive power dispatch problem: A comparative study," *Inf. Sci.*, vol. 278, pp. 231–249, Sep. 2014.

[27] M. Ghasemi, J. Aghaei, E. Akbari, S. Ghavidel, and L. Li, "A differential evolution particle swarm optimizer for various types of multi-area economic dispatch problems," *Energy*, vol. 107, pp. 182–195, Jul. 2016.

[28] A. Bhattacharya and P. K. Chattopadhyay, "Application of biogeography-based optimisation to solve different optimal power flow problems," *IET Gener., Transmiss. Distrib.*, vol. 5, no. 1, pp. 70–80, 2011.

[29] A. M. Shaheen, R. A. El-Sehiemy, and S. M. Farrag, "Solving multi-objective optimal power flow problem via forced initialised differential evolution algorithm," *IET Gener., Transmiss. Distrib.*, vol. 10, no. 7, pp. 1634–1647, May 2016.

[30] H. Singh and L. Srivastava, "Recurrent multi-objective differential evolution approach for reactive power management," *IET Gener., Transmiss. Distrib.*, vol. 10, no. 1, pp. 192–204, Jan. 2016.

[31] K. Abaci and V. Yamacli, "Differential search algorithm for solving multi-objective optimal power flow problem," *Int. J. Electr. Power Energy Syst.*, vol. 79, pp. 1–10, Jul. 2016.

[32] M. Basu, "Multi-objective optimal reactive power dispatch using multi-objective differential evolution," *Int. J. Electr. Power Energy Syst.*, vol. 82, pp. 213–224, Nov. 2016.

[33] W. Warid, H. Hizam, N. Mariun, and N. Abdul-Wahab, "Optimal power flow using the Jaya algorithm," *Energies*, vol. 9, no. 9, p. 678, Aug. 2016.

[34] S. Li, W. Gong, L. Wang, X. Yan, and C. Hu, "Optimal power flow by means of improved adaptive differential evolution," *Energy*, vol. 198, May 2020, Art. no. 117314.

[35] E. Naderi, M. Pourakbari-Kasmaei, F. V. Cerna, and M. Lehtonen, "A novel hybrid self-adaptive heuristic algorithm to handle single- and multi-objective optimal power flow problems," *Int. J. Electr. Power Energy Syst.*, vol. 125, Feb. 2021, Art. no. 106492.

[36] S. Li, W. Gong, L. Wang, and Q. Gu, "Multi-objective optimal power flow with stochastic wind and solar power," *Appl. Soft Comput.*, vol. 114, Jan. 2022, Art. no. 108045.

[37] H. T. Kahraman, M. Akbel, and S. Duman, "Optimization of optimal power flow problem using multi-objective manta ray foraging optimizer," *Appl. Soft Comput.*, vol. 116, Feb. 2022, Art. no. 108334.

[38] M. H. Nadimi-Shahraki, A. Fatahi, H. Zamani, S. Mirjalili, and D. Oliva, "Hybridizing of whale and moth-flame optimization algorithms to solve diverse scales of optimal power flow problem," *Electronics*, vol. 11, no. 5, p. 831, Mar. 2022.

[39] A. A. Mohamed, S. Kamel, M. H. Hassan, M. I. Mosaad, and M. Aljohani, "Optimal power flow analysis based on hybrid gradient-based optimizer with moth-flame optimization algorithm considering optimal placement and sizing of FACTS/wind power," *Mathematics*, vol. 10, no. 3, p. 361, Jan. 2022.

[40] R. Storn and K. Price, "Differential evolution—A simple and efficient heuristic for global optimization over continuous spaces," *J. Global Optim.*, vol. 11, pp. 341–359, Dec. 1997.

[41] Sk. M. Islam, S. Das, S. Ghosh, S. Roy, and P. N. Suganthan, "An adaptive differential evolution algorithm with novel mutation and crossover strategies for global numerical optimization," *IEEE Trans. Syst., Man, Cybern., B, Cybern.*, vol. 42, no. 2, pp. 482–500, Apr. 2012.

[42] F. Lezama, G. Castañón, and A. M. Sarmiento, "Routing and wavelength assignment in all optical networks using differential evolution optimization," *Photonic Netw. Commun.*, vol. 26, nos. 2–3, pp. 103–119, Dec. 2013.

[43] R. D. Zimmerman, C. E. Murillo-Sánchez, and R. J. Thomas, "MATPOWER: Steady-state operations, planning, and analysis tools for power systems research and education," *IEEE Trans. Power Syst.*, vol. 26, no. 1, pp. 12–19, Feb. 2011.

[44] C. E. Murillo-Sánchez, R. D. Zimmerman, C. L. Anderson, and R. J. Thomas, "Secure planning and operations of systems with stochastic sources, energy storage, and active demand," *IEEE Trans. Smart Grid*, vol. 4, no. 4, pp. 2220–2229, Dec. 2013.

[45] Yarpiz Team. (Feb. 2019). *Nature-Inspired Algorithms*. Web Page. [Online]. Available: https://www.yarpiz.com

[46] J. Sarda, K. Pandya, and K. Y. Lee, "Dynamic optimal power flow with cross entropy covariance matrix adaption evolutionary strategy for systems with electric vehicles and renewable generators," *Int. J. Energy Res.*, vol. 45, no. 7, pp. 10869–10881, Jun. 2021.

[47] P. Biswas, P. Suganthan, and G. Amaratunga, "Optimal power flow solutions using algorithm success history based adaptive differential evolution with linear population reduction," in *Proc. IEEE Int. Conf. Syst., Man, Cybern. (SMC)*, Oct. 2018, pp. 249–254.

[48] F. Lezama, J. Soares, R. Faia, T. Pinto, and Z. Vale, "A new hybrid-adaptive differential evolution for a smart grid application under uncertainty," in *Proc. IEEE Congr. Evol. Comput. (CEC)*, Jul. 2018, pp. 1–8.

[49] F. Lezama, J. Soares, R. Faia, and Z. Vale, "Hybrid-adaptive differential evolution with decay function (HyDE-DF) applied to the 100-digit challenge competition on single objective numerical optimization," in *Proc. Genetic Evol. Comput. Conf. Companion*, New York, NY, USA, Jul. 2019, pp. 7–8.

[50] H. I. Shaheen, G. I. Rashed, and S. J. Cheng, "Optimal location and parameter setting of UPFC for enhancing power system security based on differential evolution algorithm," *Int. J. Electr. Power Energy Syst.*, vol. 33, no. 1, pp. 94–105, Jan. 2011.

[51] G. I. Rashed, Y. Sun, K. A. Rashed, and H. I. Shaheen, "Optimal location of unified power flow controller by differential evolution algorithm considering transmission loss reduction," in *Proc. IEEE Int. Conf. Power Syst. Technol. (POWERCON)*, Oct. 2012, pp. 1–6.

[52] B. Mahdad and K. Srairi, "Adaptive differential search algorithm for optimal location of distributed generation in the presence of SVC for power loss reduction in distribution system," *Eng. Sci. Technol., Int. J.*, vol. 19, no. 3, pp. 1266–1282, Sep. 2016.

[53] B. Poornazaryan, P. Karimyan, G. B. Gharehpetian, and M. Abedi, "Optimal allocation and sizing of DG units considering voltage stability, losses and load variations," *Int. J. Electr. Power Energy Syst.*, vol. 79, pp. 42–52, Jul. 2016.

[54] V. Loia, A. Vaccaro, and K. Vaisakh, "A self-organizing architecture based on cooperative fuzzy agents for smart grid voltage control," *IEEE Trans. Ind. Informat.*, vol. 9, no. 3, pp. 1415–1422, Aug. 2013.

[55] A. Vaccaro, G. Velotto, and A. F. Zobaa, "A decentralized and cooperative architecture for optimal voltage regulation in smart grids," *IEEE Trans. Ind. Electron.*, vol. 58, no. 10, pp. 4593–4602, Oct. 2011.

[56] I. Khan, Z. Li, Y. Xu, and W. Gu, "Distributed control algorithm for optimal reactive power control in power grids," *Int. J. Electr. Power Energy Syst.*, vol. 83, pp. 505–513, Dec. 2016.

[57] S. M. Abdelkader, "Characterization of transmission losses," *IEEE Trans. Power Syst.*, vol. 26, no. 1, pp. 392–400, Feb. 2011.

[58] H. Ahmadi and J. R. Martí, "Minimum-loss network reconfiguration: A minimum spanning tree problem," *Sustain. Energy, Grids Netw.*, vol. 1, pp. 1–9, Mar. 2015.
[59] S. Kalyani and K. S. Swarup, "Particle swarm optimization based K-means clustering approach for security assessment in power systems," *Expert Syst. Appl.*, vol. 38, no. 9, pp. 10839–10846, Sep. 2011.
[60] A. Trias, "The holomorphic embedding load flow method," in *Proc. IEEE Power Energy Soc. Gen. Meeting*, Jul. 2012, pp. 1–8.
[61] J. Lavaei and S. H. Low, "Zero duality gap in optimal power flow problem," *IEEE Trans. Power Syst.*, vol. 27, no. 1, pp. 92–107, Feb. 2012.
[62] A. Trias and J. L. Marín, "The holomorphic embedding loadflow method for DC power systems and nonlinear DC circuits," *IEEE Trans. Circuits Syst. I, Reg. Papers*, vol. 63, no. 2, pp. 322–333, Feb. 2016.

GERARDO CASTAÑÓN (Senior Member, IEEE) received the Bachelor of Science degree in physics engineering from the Monterrey Institute of Technology and Higher Education (ITESM), Mexico, in 1987, the Master of Science degree in physics (optics) from the Ensenada Research Centre and Higher Education, Mexico, in 1989, and the master's and Ph.D. degrees in electrical and computer engineering from The State University of New York (SUNY) at Buffalo, in 1995 and 1997, respectively. He is currently a Full Professor in electrical and computer engineering with Tecnológico de Monterrey (ITESM). He was a Visiting Scientist with the Research Laboratory of Electronics, MIT, from August 2015 to July 2016, working on silicon photonics integration and developing advanced telecommunication photonic devices and sensors in CMOS. He is a member of the national research system in Mexico. The Fulbright scholarship supported him through his Ph.D. studies. From January 1998 to November 2000, he was a Research Scientist working with the Alcatel USA Corporate Research Center, Richardson, TX, USA. Where he was doing research on IP over WDM, dimensioning and routing strategies for next-generation optical networks, and the design of all-optical routers. From December 2000 to August 2002, he was a Senior Researcher with Fujitsu Network Communications researching ultra high speed transmission systems. He has over 100 publications in journals and conferences and four international patents. He frequently acts as a reviewer for IEEE journals. He is a Senior Member of the IEEE Communications and Photonics Societies. He is a member of the Academy of Science in Mexico.

ALBERTO F. MARTÍNEZ-HERRERA (Member, IEEE) is currently pursuing the Ph.D. degree in information technologies and communications with Tecnológico de Monterrey (ITESM), Monterrey, Mexico. From October 2013 to October 2014, he was an invited Ph.D. student working on cryptography with the Computer Science Department, Research Center of IPN (CINVESTAV), Zacatenco, Distrito Federal, Mexico. His research interests include applied cryptography, network security systems (secure protocols and intrusion detection systems), and network topologies. He also works on efficient hardware design techniques for cryptographic primitives and their resistance against side-channel attacks.

ANA MARIA SARMIENTO (Member, IEEE) received the Bachelor of Science degree in physics engineering from the Monterrey Institute of Technology and Higher Education (ITESM), Mexico, in 1989, and the master's and Ph.D. degrees in industrial engineering from The State University of New York (SUNY) at Buffalo, in 1995 and 2001, respectively. Her dissertation research was on the integrated production-logistics network optimization for the partner-chain design in agile manufacturing. Her dissertation topic received the 1998 Doctoral Dissertation Award presented by the International Society of Logistics. From 1999 to 2001, she was with i2 Technologies, Irving, TX, USA. She has been teaching as a Lecturer Professor with the Department of Industrial Engineering, ITESM, Monterrey, since January of 2007. Her current research interest includes the application of optimization methods of operations research to telecommunication networks.

ALEJANDRO ARAGÓN-ZAVALA (Senior Member, IEEE) received the Graduate degree in electronics and communications engineering from Tecnológico de Monterrey, Campus Querétaro, in December 1991, and the M.Sc. degree in satellite communication engineering and the Ph.D. degree in antennas and propagation from the University of Surrey, in 1998 and 2003, respectively. He was an Engineer and a Consultant in the industry, and since 2003, he has been the Academic Director of the former IEC and ISE undergraduate programs with Tecnológico de Monterrey, Campus Querétaro, and he is in charge of ITE (all electronic engineering degrees). His research interests include mobile communications, satellite systems, high-altitude platform systems, antenna design, and indoor propagation.

FERNANDO LEZAMA (Senior Member, IEEE) received the Ph.D. degree in ICTs from the Monterrey Institute of Technology and Higher Education (ITESM), in 2014. Since August 2017, he has been a Researcher with GECAD-Polytechnic of Porto, where he contributes to applying computational intelligence (CI) in the energy domain under various problems. He has published over 100 articles in intelligent systems, energy conferences, and SCI journals. He has also been a part of the National System of Researchers of Mexico, since 2016, the Co-Chair of the IEEE CIS TF 3 on CI in the energy domain (appointed as the Chair, from 2019 to 2021), and he has been involved in the organization of special sessions, workshops, and competitions at IEEE WCCI, IEEE CEC, and ACM GECCO, to promote the use of CI to solve complex problems in the energy domain.